Diazotrophic *Trichodesmium* impact on UV-Vis radiance and pigment composition in the South West tropical Pacific

Cécile Dupouy[1], Robert Frouin[2], Marc Tedetti[1], Morgane Maillard[1], Martine Rodier[3], Fabien Lombard[4], Lionel Guidi[4], Marc Picheral[4], Jacques Neveux[5], Solange Duhamel[6], Bruno Charrière[7], and Richard Sempéré[1]

[1]Aix Marseille Université-CNRS-INSU, IRD, Mediterranean Institute of Oceanography (MIO), UM 110, IRD Nouméa BP A5, 98848 Nouméa Cedex, New Caledonia
[2]Scripps Institution of Oceanography, University of California San Diego, La Jolla, CA 92093-0224, USA
[3]EIO (Ecosystèmes Insulaires Océaniens), Institut de Recherche pour le Développement-Université de la Polynésie Française-Institut Malarmé-Ifremer, Papeete, French Polynesia
[4]Sorbonne Universités, UPMC Université Paris 06, CNRS, Laboratoire d'Océanographie de Villefranche (LOV), Observatoire Océanologique, 06230 Villefranche-sur-Mer, France
[5]Observatoire Océanologique de Banyuls, CNRS-UPMC, LOMIC (UMR 7621), Avenue Pierre Fabre, 66650 Banyuls sur Mer, France
[6]Lamont Doherty Earth Observatory, Columbia University, Palisades, New York, USA
[7]CNRS, Cefrem, Université de Perpignan. 52, av. Paul Alduy 66860, Perpignan Cedex, France

Correspondence: Cécile Dupouy (cecile.dupouy@ird.fr)

Abstract.

We assessed the influence of the marine diazotrophic cyanobacterium *Trichodesmium* on the bio-optical properties of South West Tropical Pacific waters (18-22°S, 160°E-160°W) during the February-March 2015 OUTPACE cruise. We performed measurements of backscattering and absorption coefficients, irradiance, and radiance in the euphotic zone with a Satlantic MicroPro free-fall profiler and took Underwater Vision Profiler 5 (UPV5) pictures for counting the largest *Trichodesmium* spp. colonies. Pigment concentrations were determined by fluorimetry and high performance liquid chromatography and picoplankton abundance by flow cytometry. Trichome concentration was estimated from pigment algorithms and validated by surface visual counts. The abundance of large colonies counted by the UVP5 (maximum 7093 colonies m^{-3}) was well correlated to the trichome concentrations (maximum 2093 trichomes L^{-1}) with an aggregation factor of 600. In the Melanesian Archipelago, a maximum of 4715 trichomes L^{-1} was enumerated in pump samples (3.2 m) at 20°S 167 30°E. Large *Trichodesmium* abundance was always associated with peaks of mycosporine-like amino acids in the particulate absorption spectrum (330, 360 nm) and high particulate backscattering, but not with high Chla fluorescence or high chlorophyll-a concentration, or blue particulate absorption (440 nm). Along the West-to-East transect, *Trichodesmium* together with *Prochlorococcus* represented the major part of total chlorophyll concentration; the contribution of other groups revealed relatively small or negligible. The *Trichodesmium* contribution to total chlorophyll concentration was the highest in the Melanesian Archipelago around New Caledonia and Vanuatu (60%), progressively decreased to the vicinity of the Fiji Islands (30%), and reached a minimum in the South Pacific gyre where *Prochlorococcus* dominated chlorophyll concentration. The contribution of *Trichodesmium* to zeaxanthin was respectively 50, 40, and 20% for these regions. During the OUTPACE cruise, the relationship between nor-

1

malized water-leaving radiance (nLw) in the ultraviolet and visible and chlorophyll concentration was similar to that found during the BIOSOPE cruise in the Eastern tropical Pacific. Principal component analysis (PCA) of OUTPACE data showed that nLw at 305, 325, 340, 380, 412, and 440 nm was strongly correlated to chlorophyll and zeaxanthin, while nLw at 490 and 565 nm exhibited lower correlations. These results, as well as differences in the PCA of BIOSOPE data, indicated that nLw variability in the greenish blue and yellowish green during OUTPACE was influenced by other variables associated with *Trichodesmium* presence, such as backscattering coefficient, phycoerythrin fluorescence, and/or zeaxanthin absorption, suggesting that *Trichodesmium* detection should involve examination of nLw in this spectral domain.

1 Introduction

The ecological importance of filamentous diazotrophs (*Trichodesmium* spp. in particular) in the archipelago region of the South West Tropical Pacific (SWTP) has been suspected for long (Dandonneau and Gohin, 1984; Dupouy et al., 1988; 1990; 1992). *Trichodesmium* spp. have to be taken into account for estimating the global oceanic nitrogen and carbon fluxes (Capone and Carpenter, 1997; Bonnet et al., 2017; Dutheil et al., this issue). In the past decade, efforts have been made to extract abundances of different autotrophic groups from ocean color data (Blondeau-Patissier et al., 2014; Bracher et al., 2017). Other attempts have been made to get remote sensing estimates of the abundance and diazotroph activity of *Trichodesmium* at a global scale (Subramaniam et al., 2002; Westberry and Siegel, 2005; 2006;McKinna et al., 2011; Dupouy et al., 2011; McKinna, 2015). Satellite detection of *Trichodesmium* is facilitated when concentration at the sea surface is high, leading to a building of mat larger than a 300-m satellite pixel as these mats induce a high reflectance in the near infrared, a "red edge", which can easily be observed (Hu et al., 2010; Dupouy et al., 2011; McKinna et al., 2011; Gower et al., 2014; McKinna, 2015; Rousset et al., this issue). Detection becomes more difficult when *Trichodesmium* concentrations are at non-bloom or sub-bloom abundance, i.e., when colonies are distributed throughout the water column and mixed with other species. Using an empirical statistical approach, De Boissieu et al. (2014) determined that at sufficient concentration level, these filamentous diazotrophs could be distinguished from other groups. This complements empirical parameterizations that were used to derive the vertical distribution of different phytoplankton groups (micro-, nano-, and picoplankton) using High Performance Liquid Chromatography (HPLC) diagnostic pigments and surface chlorophyll-a concentration (Chla) determined from space (Uitz et al., 2006; Ras et al., 2008; Brewin et al., 2011).

In order to validate *Trichodesmium* discrimination algorithms, and to improve the knowledge of the influence of *Trichodesmium* spp. on apparent (AOPs) and inherent (IOPs) optical properties of seawater, accurate field determinations of these properties are required. Among AOPs, normalized water-leaving radiance $nL_w(\lambda)cm^{-2}sr^{-1}$, the radiance that emerges from the ocean in the absence of atmosphere, with the Sun at zenith, at the mean Earth-Sun distance (Gordon, 2005), is governed by two main IOPs (Mobley 1994; Kirk, 1994): volume absorption [$a(\lambda)$in m^{-1}] and volume backscattering [b_b in m^{-1}] coefficients. IOPs are controlled by the concentrations of optically active components in a volume of water, which include phytoplankton and colored detrital matter (CDM), the latter being composed by non algal particulate matter (NAP) and chromophoric dissolved organic matter (CDOM). If AOPs are well related to phytoplankton pigments in Case I oceanic waters (Morel and Maritorena,

2001; Morel et al., 2007), this relationship might be modified by the presence of *Trichodesmium* (with moderate Chla concentrations < 1 mg m^{-3}). As summarized in Westberry and Siegel (2005), *Trichodesmium* displays unique optical properties that may allow their detection: (1) a strong absorption in the ultraviolet (UV) domain related to the presence of mycosporin like amino-acids (MAAs) (Subramaniam et al., 1999a; Dupouy et al, 2008), (2) a higher relative reflectance near 570 nm due to phycoerythrin fluorescence (Borstad et al., 1992; Subramaniam et al., 1999b), and (3) increased backscattering across all wavelengths caused by the change in refraction index of intracellular gas vacuoles (Borstad et al., 1992; Subramaniam et al., 1999b; Dupouy et al., 2008).

The SWTP between New Caledonia and the Tonga trench is particularly rich in *Trichodesmium* colonies during summer (Dupouy et al., 1988; 2000; 2011; Biegala et al., 2014) and this richness further enhanced during the positive phase of the ENSO in 2003 (Tenorio et al., 2018). Using bio-optical measurements, this study aims (1) to describe several AOPs and IOPs of interest in the UV and visible domains of SWTP waters, as well as pigments, and abundance of all phytoplanktonic cells including large and smaller *Trichodesmium* colonies and picoplankton, (2) to determine the influence of *Trichodesmium* spp. on in situ measurements of ocean color, and absorption and backscattering coefficients. For this purpose, we used identical measurements than those made in the tropical oligotrophic ocean during the BIOSOPE cruise (Tedetti et al., 2007; 2010).

2   Material and methods

2.1   Study area

The "Oligotrophy from Ultra-oligoTrophy PACific Experiment (OUTPACE)" cruise was conducted on board R/V L'Atalante from 21 February to 31 March 2015 in the SWTP (Table 1; Fig. 1). *In situ* measurements and water sampling were performed at fifteen stations along a 4000-km transect. This transect extended from the mesotrophic waters of the Melanesian Archipelago (MA: SD1 to SD6) near New Caledonia and Vanuatu, to the Fijian archipelago between Fiji and Tonga (FI: SD7 to SD12), and to the eastern end in the hyper-oligotrophic waters of the South Pacific gyre, East of Tonga Trench (SPG: SD13 to SD15). In addition, three long duration stations A, B, and C were sampled during 7 days in each of these three regions (LDA in MA, LDB in FI, and LDC in SPG; Fig. 1). General biogeochemical and hydrographic characteristics of the waters along this transect are described in Moutin et al. (2018).

2.2   Radiometric measurements and determination of $K_d(\lambda), K_d(\lambda)$ and $Z10\%(\lambda)$ values

At each station, two or more profiles of downward irradiance [$E_d(Z, \lambda)$] in μW cm^{-2}nm^{-1}] and upward radiance [$L_u(Z, \lambda)$] in μW cm^{-2}nm^{-1}] were made around solar noon using a Satlantic MicroPro free-fall profiler equipped with OCR-504 downward irradiance and upward radiance sensors with UV-B (305 nm), UV-A (325, 340 and 380 nm) and visible (412, 443, 490 and 565 nm) spectral channels, as further described in Tedetti et al. (2010). The MicroPro profiler was operated from the rear

of the ship and deployed 30 m away to minimize the disturbances of the ship. Surface irradiance [$E_s(\lambda)$] in μW cm^{-2}nm^{-1}] was concomitantly measured at the same wavelengths on the ship deck using other OCR-504 sensors to take into account the short-time variations of cloud conditions during the cast. Surface and in-water radiometers were calibrated before the cruise. Mostly, cloudy sky conditions existed during the profiles (only a few acquisitions were made under clear skies), and at SD5 at 17:30-19:00, they were made under a heavy shower. SD3, SD4, and SD13 profiles were not available (night stations). Details of the casts can be found in Appendix A. For the $nL_w(\lambda)$ of the long duration stations, an average on 7 days was calculated as representative of the station, with coefficients of variation of 12-14% at LDA, 6-9% at LDB (without day 4), and 2.5% at LDC. Diffuse attenuation coefficient for downward irradiance ($K_d(\lambda)$in m^{-1}) was determined using $E_d(Z,\lambda)$and $E_s(\lambda)$ values (Appendix A). The first optical depth corresponding to the surface layer observed by the satellite ocean color instruments (Kirk, 1994) [Z10% (λ) in m] was extrapolated from $K_d(\lambda)$ and calculated as $\ln(10)/K_d(\lambda)$. Determination of $nL_w(Z,\lambda)$ was conducted from $L_u(Z,\lambda)$ values and diffuse attenuation coefficient for upward radiance [$K_L(\lambda)$in m^{-1}], within different depths according to stations and wave bands, then normalized by $E_s(\lambda)$ (see calculations in Appendix A). The $K_d(\lambda)$ data presented in this study are average values of two to three upward radiance casts (coefficient of variation < 8% for each station concerned).

2.3   Water sampling

Seawater samples were collected during the noon casts at different depths using 12-L Niskin bottles for the determination of various parameters. For the determination of Chla and particulate (phytoplankton + NAP) absorption coefficient [$a_P(\lambda)$], samples were collected at depths corresponding to different % of PAR (i.e., 75, 54, 36, 10, 1, 0.1%) and filtered [288 mL for Chla determination by fluorometry, and 2.25 L for $a_P(\lambda)$] through 25-mm Whatman GF/F filters. Then, the filters were immediately stored in liquid N2 (-196°C) in Nunc® cryogenic vials until analysis. Samples were also collected at all depths for liposoluble HPLC pigment analyses (see LOV laboratory data, OUTPACE database, J. Ras). In addition, samples for HPLC pigments were taken in duplicate at surface and Deep Chlorophyll Maximum (DCM) as part of a NASA satellite validation program. For this, 3 to 4.5 L of seawater was filtered onto 25-mm Whatman GF/F filters, which were further stored in liquid N2 until analyses at NASA. Water-soluble pigment (phycoerythrin, PE) concentration was determined for the >10 μm size fraction. Therefore 4.5 L of seawater was filtered onto 47-mm Nuclepore filters with pore sizes 10 μm and stored in liquid N2 in Nunc® cryogenic vials (PE > 10 μm). Filters were preserved (at -80°C) until analysis in the laboratory (IRD French Polynesia).

For the determination of picoplanktonic population abundances (Bock et al., 2018), water samples were fixed with paraformaldehyde (final concentration of 0.2%) immediately after sampling, flash frozen in liquid nitrogen, and stored in liquid N2 in Nunc® cryogenic vials until analysis, and abundance at 5 meters were selected for our study. For the determination of CDOM absorption, 200 mL of seawater were immediately filtered on Micropore filters of 0.2 μm pore size using Nalgene filtration units previously rinsed twice with HCL and stored in SCHOTT® glass bottles, previously combusted (450 °C, 6 h) and rinsed twice with HCL. Pump samples (depth of 3.5 m) were also collected all along three transects in order to increase the frequency of both pigments and IOPs' surface measurements (Chla, HPLC-NASA) in areas characterized by important *Trichodesmium* surface slicks: the "Simbada" transect, with 7 samples between SD3 and SD4 in the MA, the High Frequency HF1 transect (31

4

samples) in the MA near LDA, and the High Frequency HF2 transect in the FI near LDB (42 samples). Besides radiometric measurements and water sampling, in situ measurements were also performed for the determination of *Trichodesmium* spp. colonies and backscattering coefficients (see below).

2.4 FTL$_{Tricho}$ abundance: large *Trichodesmium* spp. colonies

An Underwater Vision Profiler 5 (UVP5), serial number Sn003, pixel size ca. 0.147 mm x 0.147 mm (Picheral et al., 2010) was coupled to the metal structure of the CTD. The device emitted flashes of red LED light that illuminates 0.95 L of water. Images of all particles within the illuminated area were recorded and analyzed in terms of abundances of defined size ranges. Objects larger than 30 pixels were saved and uploaded on ecotaxa (http://ecotaxa.obs-vlfr.fr/prj/37) and further determined on board as Trichodesmium colonies of fusiform and round-shaped colonies of all sizes. From 190074 objects recovered, 100342 were identified as "fiber tricho like *Trichodesmium*" (FTL$_{Tricho}$), i.e., all particles of *Trichodesmium* with fusiform-shape (tuff form) and round-shape (puff form) colonies from > 200 μm to 2-5 mm in size. FTL_{Tricho} is assumed to be mostly *Trichodesmium* colonies with a possible risk that a small quantity of fibers could instead be diatoms chains. Contrary to a classical counting at the microscope, no abundance of free filaments is available, although these filaments represent often a significant part of the *Trichodesmium* assemblage (Carpenter et al., 2004). The FTL$_{Tricho}$ abundance is expressed in Colonies per m^{-3} and measured at 5-m depth intervals (Picheral et al., 2010) providing FTL$_{Tricho}$ "vertical concentrations" at each cast. The FTL$_{Tricho}$ abundance at 5-m depth was generally underestimated compared to that at 10-m and 15-m depths (possibly due to smaller size of colonies). Therefore, the value at 10 m was selected as representative of the abundance of the surface layer. As different FTL$_{Tricho}$ abundance profiles were acquired during the day (from 1 to 5 depending on the station), a daily average of the 10-m FTL$_{Tricho}$ abundance was made. Daily average, maximum value of the day, and the FTL$_{Tricho}$ abundance at noon (i.e., the nearest from the time of the Satlantic radiometric profile) were compared and showed no statistical difference. For the three long duration stations, an average on 7 days of the 10 m-FTL$_{Tricho}$ abundance and a variation coefficient were calculated.

In order to estimate a trichome concentration, photographs taken with a Dino-Lite hand-held Digital Microscope covering the totality of the filtered surface on the GF/F filters dedicated to absorption measurements were used. Colonies were first visually enumerated. The uncertainty on this colony and isolated filaments (essentially *Katagnymene*) visual enumeration was estimated at 10%. The trichome concentration (L^{-1}) was estimated using a constant number of 10 trichomes per colony as representative of an average of each size class and shapes).

2.5 Picoplankton

Picoplankton population abundances were estimated by flow cytometry using a BD Influx flow cytometer (BD Biosciences, San Jose, CA, USA). *Prochlorococcus* (Proc), *Synechochoccus* (Syn) and picoeucaryotes (Peuk) were enumerated using the red and orange fluorescence, while non-pigmented bacteria and protist groups were discriminated in a sample aliquot stained with SYBR Green I DNA dye, as described in Bock et al. (this issue). Using a forward scatter detector with the "small par-

ticle option" and focusing at 488 and 457 nm (200 and 300 mW solid state, respectively) laser into the same pinhole greatly improved the discrimination between the dim signal from Proc at the surface and background noise in unstained samples. Nanoeucaryotes (Neuk) were not further differentiated from Peuk. Cell abundances of Proc, Syn, Peuk and bacteria showed a vertical and uniform abundance distribution due to their mixing in the 0-30 m layer (Bock et al., this issue).

5

2.6 Chlorophyll a, phycoerythrin and pigment analyses

For Chla determination by the fluorimetric method, filters were extracted with 5 mL methanol in darkness over a 2 h period at 4 °C and quantified using a Trilogy Turner fluorometer according to Le Bouteiller et al. (1992). HPLC pigments analysis on surface and DCM samples were performed according to the NASA protocol and provided monovinyl-Chla (MV-Chla), divinyl-Chla (DV-Chla), accessory chlorophylls, and photosynthetic and photoprotective carotenoids (Hooker et al., 2012). PE was extracted in 50/50 glycerol/phosphate buffer. Quantification of this pigment was obtained from the area below the fluorescence excitation curve, using a calibrating procedure previously described (Wyman, 1992; Lantoine and Neveux 1997; Neveux et al., 2006). Furthermore, pigment ratios were also used to estimate the relative importance of pico-, nano-, and micro-plankton in terms of Chla using relative contributions of different accessory pigments divided by the sum of accessory pigments (Ras et al., 2008). The proportion of Proc to total Chla (TChla) was estimated from the DV-Chla/TChla ratio. It usually represents a high proportion due of its high abundance despite of its small size (Grob et al., 2008).

2.7 Algorithms for *Trichodesmium* abundance estimates using pigments

As a true microscopic determination of *Trichodesmium* abundance was not carried out at each station during the OUTPACE cruise, we used algorithms to derive trichome abundances from pigment concentrations (chlorophylls, zeaxanthin, PE > 10 μm and flow cytometric cell counting. Using a constant PE concentration per trichome (196 pg trichome^{-1}) and a constant Chla per trichome (100 pg cell^{-1}) as in Tenorio et al. (2018), calculations of trichome concentration (L^{-1}) could be done both from PE or Chla > 10 μm, assuming that other autotrophic organisms have a negligible contribution in this large size fraction. As Chla > 10 μm was not available for OUTPACE, Total MV-Chla was used, which corresponds to the sum of Chla from Syn and *Trichodesmium*, and all eukaryotic phytoplankton cells (pico-, nano-, and microphyto-plankton). MV-Chla associated with Syn and Peuk was estimated at the surface using measured cell concentrations and the Chla per cell values obtained on cultures grown at high light intensity (Laviale and Neveux, 2011), i.e., 1.2 fg cell^{-1} for Syn and 10 fg cell^{-1} for Peuk (assuming a concentration intermediate between the one of *Micromonas pusilla* and *Ostreococcus*). Peuk included also Neuk, and neglecting the rest of phytoplankton (larger cells, see Leblanc et al., this issue). Microplankton biomass other than *Trichodesmium* was not significant at OUTPACE (Leblanc et al., this issue). MV-Chla from Syn+Peuk including Neuk was then deduced from Total MV-Chla to obtain MV-Chla associated to *Trichodesmium*. The *Trichodesmium* spp. abundance was also estimated from total zeaxanthin (TZea). For this, Zea per Proc cell (Zea-Proc) was determined in the area where *Trichodesmium* is absent and assuming a constant Zea concentration per Syn cell (Zea-Syn) determined on Syn cultures at high light intensity (Laviale

6

and Neveux, 2011). The Zea *Trichodesmium* was then deduced by substracting Zea-(Proc+Syn) from Tzea (Zea associated to chlorophytes being considered as negligible). *Trichodesmium* abundance was deduced from Zea concentration per colony found in Carpenter et al. (1993). We compared then estimations of *Trichodesmium* from these pigment algorithms to FTL_{Tricho} abundance and trichome concentration estimated from visual counts.

5

2.8   Particulate and CDOM absorption, backscattering measurements

Light absorption spectra were measured directly with filters soaked in filtered seawater, by referencing them to an equally soaked empty filter. Measurements were done in single-beam Beckman DU-600 spectrophotometer after soaking frozen filters with filtered sea water. Absorbance (optical density) spectra were acquired between 300 and 800 nm in 2-nm steps. To correct the pathlength amplification effect on filters, the optical density of the equivalent Suspension, (ODs), was obtained from the Optical Density on Filter, (ODf), as ODs= A ODf + B $(ODf)^2$ with A and B coefficients determined by Mitchell et al. (1990) as used in oligo- to mesotrophic waters in the Pacific ocean (Dupouy et al., 1997; 2003; 2010). All spectra were shifted to zero in the infrared by subtracting the average optical density between 750 and 800 nm. Optical densities were finally converted into the total particulate absorption coefficients [a$_P(\lambda)in$m^{-1}]. The a$_P$(330) to a$_P$(676) ratio was calculated as photoprotection index related to MAAs (330 nm: absorption maximum of shinorine) in total phytoplankton (676 nm, absorption maximum of Chla), as in Ferreira et al. (2013). CDOM absorption spectra were measured on board with a 200-cm pathlength liquid waveguide capillary cell (LWCC, WPI) as described in Martias et al. (2018). A broad peak around 350 nm was visible in most of the CDOM spectra, except for LDB and SPG stations (not shown).

Backscattering coefficients were determined with the default correction (σ) applied to compensate for the loss of photons absorbed by the medium between the instrument and the detection volume as described in Dupouy et al. (2010) from a Hydroscat 6 (HOBILabs, Inc) at 6 wavelengths (412, 442, 510, 550, 620 and 676 nm). The particulate backscattering [$b_{bp}(\lambda)m^{-1}$] was obtained by subtracting the backscattering coefficient of pure water, bbw (Morel, 1988). Due to an electronical shortage inside the instrument, only stations SD1 to SD6 and LDA-days 1-5, were available and no station were sampled after SD6. Backscattering coefficients of surface oligotrophic waters (SD13, LDC, SD14, SD15), which are supposed to depend deeply on TChla according to Huot et al. (2008) for the South East Pacific, were deduced from Chla using a Look-Up Table of data obtained during DIAPALIS (DIAzotrophy in the Pacific on ALIS) cruises in the Loyalty Channel (Dupouy et al., 2010).

2.9   Statistics

Ocean Data View sections Schlitzer, R., Ocean Data View, http://odv.awi.de, 2016 was employed for the spatial representation of biogeochemical parameters over the vertical (0-150m). The spatial interpolation/gridding of data was performed using Data-Interpolating Variational Analysis (DIVA). Principal component analyses (PCA) were conducted on the basis of Pearson's correlation matrices using XLSTAT 2011.2.05.

3 Results

3.1 Distributions of $\mathrm{nL}_w(\lambda), \mathrm{K}_d(\lambda)$ and $Z10\%(\lambda)$

Along the OUTPACE transect, $\mathrm{nL}_w(\lambda)$ showed a large range of values and spectral shape (Fig. 2a). In the UV (305-380 nm), violet (412 nm), and blue (443 and 490 nm), $\mathrm{nL}_w(\lambda)$ were the lowest in the MA, increasing towards the SPG (SD14-SD15, LDC). For all the wavebands, with the exception of the yellowish green one (565 nm), $\mathrm{nL}_w(\lambda)$ at SD14 and LDC was higher than the 90th percentile, and $\mathrm{nL}_w(\lambda)$ at SD9 and LDB were lower than the 10th percentile (Fig. 2a). Values of $\mathrm{nL}_w(\lambda)$ in this violet-blue domain were similar than those measured in the most oligotrophic oceanic areas at the Eastern part of the OUT-PACE transect (Tedetti et al., 2010). For example, in the center of the SPG during BIOSOPE cruise (20-30 °S, 142-126°W), $\mathrm{nL}_w(412), nL_w(443)$, and $\mathrm{nL}_w(490)$ reached up to 4.5, 4, and 2 $\mu\mathrm{Wcm}^{-2}\mathrm{nm}^{-1}\mathrm{sr}^{-1}$, respectively for TChla concentrations < 0.022 mg m^{-3} and with a DCM at 180 m. The frontal station LDB at OUTPACE exhibited a peculiar spectrum with waters greener than all other stations (Fig. 2b). The low nL_w corresponded to a high TChla concentration of 0.43 mg m^{-3} formed by *Trichodesmium* and picoplankton on a surface physical front (Rousselet et al., this issue). Moreover, the GF/F filters used for absorption at these stations showed an orange-yellow color when observed under the Dino-Lite microscope. Such color was not observed in the MA, and is typical of small picoplanktonic cells as Pro and Syn.

For all stations, [$\mathrm{K}_d(\lambda)$ decreased from the UV-B to UV-A spectral domain (Table 1). From the MA to the FI, $\mathrm{K}_d(\lambda)(325)$ was high from SD1 to SD6, then decreased from SD7 to SD12, and showed a peak at LDB, and minimum at the SPG stations. During the 5-day long duration stations, $\mathrm{K}_d(325)$ variations (not shown) reflected those of TChla with values decreasing from day 1 to 5 at LDA (0.11 to 0.09 m^{-1}) and LDB (0.13 to 0.11 m^{-1}) and remained stable at LDC (0.05 m^{-1}). $\mathrm{K}_d(PAR)$ showed the same tendency at LDA and LDB (0.028 to 0.023 m^{-1}), and LDC (0.020 m^{-1}). These typical low values of $\mathrm{K}_d(PAR)$ in oligotrophic waters were associated to DCMs at 125, 165, 110 and 135 m and a TChla concentration of 0.036, 0.045, 0.048 and 0.023 mg m^{-3} measured at SD13-SD14-SD15 and LDC, respectively. Such values are close to that found in the South East Pacific during BIOSOPE cruise (08-35°S, 142-73°W) (Tedetti et al., 2007) and much lower than that reported for the oligotrophic waters of NW Mediterranean Sea (Sempéré et al., 2015). Maxima of $Z10\%(380)$ (Table 1; Fig. 3) were found in the FI in the oligotrophic part of the transect (LDC and SD15, 100-120 m, for a TChla concentration of 0.02 mg m^{-3}) and were comparable to those reported for the clearest natural waters in SPG (Tedetti et al., 2007). Conversely, stations exhibiting the lowest $Z10\%$ (SD1, 40 m) were found in the MA and also at the frontal station LDB in the FI (DCM of 41 m, TChla = 0.433 mg m^{-3}). The 1st optical depth determined in the UV-visible varied from 13 m (LDB-day 3) to 28 m (SD14).

3.2 Pigment composition and abundance of phytoplanktonic groups

3.3 FTL_{Tricho} abundance derived from Underwater Vision Profiler

The UVP5 FTL_{Tricho} abundance showed a wide range of values along the transect SD1-SD15 (Fig. 4a; Table 1). It was essentially concentrated in the upper 50 m although some colonies were still visible below. The maximum was obtained at SD1

(at 10m, 7663 colonies m^{-3}) and rapidly dropped to 2000 colonies m^{-3} at SD2 to stabilize between 200 and 500 colonies m^{-3} at the east of SD4. It progressively decreased from West to East. Still visible at SD5 (170°E), it vanished at SD7, where the maximum of FTL$_{Tricho}$ abundance was located deeper and finally disappeared between SD8 and SD11. On the first day of LDB, an exceptional high value of 3700 colonies m^{-3} was observed. During the long duration stations, average (CV) of 10-m *Trichodesmium* abundance was 1000 m^{-3} (35%) at LDA, 1726 m^{-3} (9%) at LDB, and 2 m^{-3} (1%) at LDC, respectively. FTL$_{Tricho}$ abundance allowed one to define 3 groups of stations, according to the log10 of abundance. The 1st group was composed by the stations SD1 to SD7, and included both LDA in the western MA and LDB in the FI (log10 > 2.8). The 2nd group was composed by SD3, and SD8 to SD12 with medium concentrations (2 < log10 < 2.8). Finally, the 3rd group contained the stations SD13, SD14, LDC, and SD15 characterized by no or very low FTL$_{Tricho}$ abundance (log10 < 2).

3.4 Picoplankton abundance and influence on TChla biomass

Picoplankton predominance was typical of oligotrophic waters (Neveux et al., 1999; Buitenhuis et al., 2012; Bock et al., this issue). The Syn abundance was particularly high in the surface layer in the MA at SD3-LDA (> 22 $10^3 cells$mL^{-1}) until the intermediate area of the Fijian basin. However, the Syn surface maximum was observed at LDB (> 100 10^3cellsmL^{-1}), together with Proc abundance peaking at LDB with more than 9 10^5cellsmL^{-1} in the upper surface layer and a small Peuk abundance of 850 cell mL^{-1}. Note that the Peuk abundance was high (> 3000 cells mL^{-1}) at the DCM only.

3.5 Chla, PE and accessory pigments

HPLC pigment analyses revealed the occurrence of four major pigments identified as MV-Chla, DV-Chla, zeaxanthin, and β carotene. HPLC pigment concentrations from LOV were used since available for each station and depth, Fig. 4b-c. The 0-150 m section of zeaxanthin concentration, the main photoprotective carotenoid contained in all cyanobacteria (Syn, Proc + *Trichodesmium*), showed values > 0.15 mg m^{-3} in the 0-50 m layer and almost continuously from SDA to SD12. Furthermore, a strong maximum was observed at the frontal LDB (Fig. 4b). TChla-LOV and TChla-NASA (from a regression between only 5 m and DCM values) was highly correlated (TChla-LOV = 0.81 × TChla-NASA; r^2 = 0.87, p < 0.05, n =12, and zea-LOV = 0.71 × zea-NASA; r^2 = 0. 88, p < 0.05, n =12; p<0.0001) this good relation though obtained on different bottle casts. TChla section (LOV: Fig. 4c) showed high values in the MA near the islands of New Caledonia-Vanuatu (SD1 to SD6) (with a maximum of 0.352 mg m^{-3} at SD1 at 5 m), and a DCM oscillating between 70 and 110 m (Table 1), with a higher value (0.534 mg m^{-3}) and a shallower DCM (52 m) at the frontal LDB. Surface PE > 10 μm values (indicative of *Trichodesmium*) showed two spots of high concentrations (Fig. 4e). The first spot is located in the Western part of the MA (SD1 to SD5), and the second is located at LDB. PE > 10 μm was low in the central part of the transect (between SD6 and SD12), and was near 0 in the SPG. Higher surface values of TChla and PE > 10 μm at LDA and LDB (Fig. 4d,e) were obtained from pump samples, and provided higher values than surface Niskin samples.

DV-Chla of Proc at the surface (Fig. 5a) tended to increase from West to East until a prominent maximum of 0.18 mg m^{-3}

at the frontal LDB, and showed minimum concentrations, higher to the East, in the SPG. It represented 22% of TChla in the MA, 39 % in the FI, and up to 39% in the SPG (and 45% at LDB). The estimates of MV-Chla in *Trichodesmium* populations (Tricho-Chla) using pigment algorithm (see Section 2.6) were between 0.10 and 0.23 mg m^{-3} in the MA, around 0.03 mg m^{-3} in the FI, with a high value of 0.08 mg m^{-3} at LDB, and lower than 0.02 mg m^{-3} in the SPG (Fig. 5a). Its contribution to TChla (Fig. 5b) varied from 52% in the MA (mean of % contribution from SD1 to SD7) and 30% in the FI, and was still 23% of TChla in the SPG (SD12-LDC). Its % contribution at LDB was lower (31%) because of a high contribution of DV-Chla. Identical contributions were calculated either using LOV or NASA surface pigments. The contribution of *Trichodesmium* zeaxanthin followed roughly the same pattern, with a contribution of 53, 40, and only 3% in the MA, FI, and SPG, respectively. Note that the contributions to TChla or zeaxanthin in the SPG are indicative only, as they are calculated on values < 0.03 mg m^{-3}. The zeaxanthin contribution was lower at SD1 and was somewhat higher between SD8-SD11 than the contribution to TChla (Fig. 5b).

3.6 Trichome concentration

The *Trichodesmium* distribution at the surface deduced from visual counts, UVP5 and pigment algorithms showed grossly similar pattern (Fig. 6). However, at a given site, differences in trichome estimates could be observed according to the method used. These differences could be partly due to patchiness distribution of trichomes (and colonies) and no concomitant sampling of the different parameters. Nevertheless, significant linear correlations between trichome concentrations estimated from PE > 10 μm, or Chla-Trichome, or microscopic visual counts, and FTL$_{Tricho}$ abundance were observed (Fig. 7a). The relatively high slopes of the linear regressions (i.e. 675, 735, 529, as factors between large colonies and trichomes, from PE > 10 μm and Chla, or visual counts respectively) are explained by the fact that FTL$_{Tricho}$ counted by the UVP5 represented only the number of the largest colonies of *Trichodesmium* (without true determination of trichome number by colony). The correlation between Chla-Trichome and our microscopic visual counts (r^2 = 0.74) was also significant (Fig. 7b). A maximum of 4715 trichomes L^{-1} was enumerated on the filter during the Simbada transect from pump samples between SD3 and SD4, at 20°S 167 30°E with Tchla of 0.3 to 0.5 mg m^{-3}.

3.7 Backscattering and absorption coefficients, photoprotection index

All particulate backscattering spectra showed large troughs due to absorption maxima by particulate material in the blue (440, 480 nm) channels (Fig. 8a) as pigment absorption has been shown to influence backscattering intensity (Stramski et al., 2008). At the most concentrated *Trichodesmium* stations (slick, SD1), the backscattering coefficient (b$_{bp-H6}$) was twice higher (at 510 nm, 0.007 m^{-1}) than in the stations where they were moderately present (SD2-SD6) (as a mean at 510 nm: 0.0025 m^{-1}) compared to the value for pure water of 0.0013 m^{-1} at 510 nm (Morel et al., 2007). The slopes of the b$_{bp-H6}$ spectra calculated without the blue channels but including the 676 nm channel (i.e. from 510 to 676nm), as the latter was not biased by Chla fluorescence; Stramski et al., 2008) were in the range 0.0017 to 0.0022 m^{2}nm^{-1}, typical of large cells. The TChla-specific

backscattering coefficient was higher in slicks [0.017 m^2mg(Chla)$^{-1}$] and lower in SD3-LDA [0.006 m^2mg(Chla)$^{-1}$] near the ones determined on colonies (Dupouy et al., 2008).

The section from 0 to 150 m of b_{bp-H6} showed that the high backscattering coefficient characterizes the 0-10 m layer in the MA (no data were collected after SD6; Fig. 8b). Typical spectra of particulate absorption for *Trichodesmium*-rich waters exhibit the two MAAs absorption peaks at 330 and 360 nm with a much lower intensity for the 360nm peak (Fig. 9a). These peaks are characteristic of *in vivo* spectra (Dupouy et al., 2008) and their amplitude though enhanced by freezing (Laurion et al., 2009) has been used in many studies to show the degree of photoprotection of phytoplankton by MAAs against UV (Ferreira et al., 2013). They were not observed at the surface in low *Trichodesmium* concentrations (FTL$_{Tricho}$ abundance; Fig 9b). Sections from 0 to 150 m of a$_P$(330) and a$_P$(440) (Fig. 9c) exhibit the impact of MAAs in the upper layer at 330 nm [a$_P$(330) > 0.4m^{-1}]. At 442 nm, there is no increase on the surface layer by FTL$_{Tricho}$ and the highest values are rather linked to the DCM at 80 m [a$_P$(440) > 0.2 m-1]. A reasonable relationship (Fig. 10a) was found between UVP-5 FTL$_{Tricho}$ abundance and a$_P$(330) when considering the entire 0-150 m layer (FTL$_{Tricho}$ abundance = 0.43 × a$_P$(330) − 2.1, r$_2$ = 0.57, n = 120, p<0.0001).

The a_P(330)/ a_P(676) ratio showed relatively high values (> 80) from 0 to 25 m, then it abruptly fell to 20 below 30-m depth (Fig. 10b). When considering the surface layer only (Fig. 10c), the MAAs index was tightly related to *Trichodesmium*, except at some stations (SD10). Indeed, MAA pigments are also produced by other phytoplankton groups (Carreto and Carignan, 2011) when exposed to high nLw(UV) values. MAA's of other groups show generally only one peak at 320 nm as in the South Eastern Pacific (Bricaud et al., 2010) or at 330 nm (large phytoplankton in the Argentina continental shelf; Ferreira et al., 2003). At OUTPACE, phytoplankton counts indicate that the contribution of other large phytoplankton (shown by the size index from HPLC pigment ratios) was low. Nevertheless, the discrepancy observed around SD10 where high values of a$_P$(330)/ a$_P$(676) ratio corresponded to low UVP5 FTL$_{Tricho}$ and visual counts could be explained by a higher concentration of other photoprotected non-cyanobacterial phytoplankton (the second peak at 360 nm was less pronounced), or a spatial heterogeneity in sampling. At LDB, the mixing with Proc decreased drastically the photoprotection index. a$_P$(330)/

3.8 Relationships between AOPs and pigments

In the present study, Chla was well correlated to all nL$_w$(λ) ratios [nL$_w$(λ)/nL_w(565)] with r^2 varying from 0.79 to 0.83 (power regressions) with RMSE (not shown) ranging from from 51 to 30% from 305 to 490 nm for OUTPACE and from 36 to 23% for BIOSOPE) according to wavelength considered (Fig. 11). The relationships between nL$_w$(λ) and Chla were different at OUTPACE than at BIOSOPE (Fig. 11). These good relationships obtained even in the UV domain, where Chla though absorbing at 380 nm does not show any absorption peak in the UV domain, were already observed in the South East Pacific during BIOSOPE cruise, for equivalent ranges, and attributed to the fact that CDM substances absorbing in the UV domain covary with Chla (Tedetti et al., 2010). The reason why the relationships are different at 305 and 325 nm wavelengths but not other UV bands (e.g., 340, 380 nm) is probably related to the presence of *Trichodesmium* and other constituent covarying with Chl and absorbing more at 305 and 325 nm than at longer UV wavelegths. It can be noted than for the same Chla, ratios are

higher at OUTPACE than at BIOSOPE, i.e. absorption would be lower in the 305 and 325 nm bands and this difference is stronger at high Chla (rich stations in the upwelling at BIOSOPE, MA stations and LDB at OUTPACE). One possible reason is that CDOM and CDM may be higher in the coastal upwelling or Marquesias waters than in the *Trichodesmium* rich-waters of OUTPACE.

3.9 Influence of *Trichodesmium* on the distribution of UV-visible nLw(λ)

To better assess the influence of *Trichodesmium* on the distribution of $nL_w(\lambda)$ values, the 8 radiances measured during the South West Pacific OUTPACE cruise (this study) and the South East Pacific BIOSOPE cruise (2004) were statistically analyzed and compared. Fig. 12a-d shows the results of a principal component analysis (PCA) operated separately on $nL_w(\lambda)$ values and TChla concentrations for the two cruises. In the South West Pacific (OUTPACE), the two principal components (PCs) represent 94% of total variance (Fig. 12b). The graph of correlations between PCs and the variables (Fig. 12a) indicates that UV and visible $nL_w(\lambda)$ are distributed along the PC1 axis, with all radiances on the right side, except 565 nm. This 1st axis (81% of total variance) indicates an effect of Chla on $nL_w(\lambda)$, with all $nL_w(\lambda)$ being higher at low Chla (blue waters) and lower at high Chla (mesotrophic waters), except at 565 nm, where on the contrary nLw increases with Chla. Oligotrophic stations are on the right side and mesotrophic stations on the left. PC2 represents 13% of the total variance. The variables that have significant correlation with PC2 are $nL_w(565)$ (Chla rich waters) and $nL_w(490)$ (Chla poor waters), both on the upper side of the PC2 axis. These different behaviors in $nL_w(565)$ and $nL_w(490)$ are significant compared to the sensitivity of the Satlantic instrument. A series of stations is positively linked to this PC2 axis (LDB4, SD1, SD2, LDA-2, SD7) while LDA-3 and LDA-4 are negatively linked to PC2. The relatively high correlation between PC2 and nLw(565), minimally influenced by Chla, suggests that other parameters than abundance (e.g., size, type) might affect $nL_w(565)$ at the stations with sizeable PC2 values. In comparison, the first 2 PCs for the South East Pacific dataset (BIOSOPE) represent 96% of the total variance, with 89% for PC1 and only 7% for PC2 (Fig. 12c). The main difference is that $nL_w(565)$ is no more linked with PC2 but only to PC1, and that for PC2 nLw(490) has an opposite behavior compared to that in the South West Pacific (correlation is negative instead of positive). At 490 nm, Chla appears to explain most of the nLw variability. This could reflect the absence of *Trichodesmium* in the Eastern Pacific. Except for a few stations, the PC2 contribution is much lower, i.e., variability is mostly described by PC1.

4 Discussion

4.1 Contribution of other phytoplankton and filamentous cyanobacteria to optical properties for interpreting satellite Chla imagery

The determination of *Trichodesmium*'s influence on IOPs compared to other microorganisms and non-living particles in the sea is a main challenge. Indeed, previous models showed that absorption is governed by size and intracellular content (Bricaud et al. 1995; 2004; 2010) and that the absorption by large *Trichodesmium* colonies suffers from a double package effect (in filaments

and in colony, Subramaniam et al., 1999a,b; Dupouy et al., 2008). Absorption by MAA's was observed on disaggregated colonies rather than on intact colonies (Fig. 3 in Subramaniam et al., 1999a), suggesting that a large fraction of MAA's is potentially present in sheaths or in the intracolony spaces. It has been shown that the highest $a_P(330)$ values in the upper layer, particularly in the western part of the MA, coincided with the highest FTL_{Tricho} (for all stations) and that the correlation was

5 significant (r2= 0.55, n = 120, p <0.0001). At the opposite, there was no correlation between $a_P(440)$ and FTL_{Tricho}. This lack of correlation is striking as *Trichodesmium* contribution to TChla is between 30 to 60% along the transect and somehow contradicts the high specific phytoplankton absorption coefficient at 440 nm found on colonies concentrated in tanks (Dupouy et al., 2008). Note that TChla measured from HPLC large volumes (4.5 L) or $a_P(440)$ (2.5 L) catches at a maximum one large FTL_{Tricho}, and that indeed in order to get a representative Trichodesmium biomass or $a_P(440)$, it would be necessary to adjust

10 filtered volumes to expected abundance (8L, Tenorio et al., 2018). This is not the case for $a_P(330)$ or $a_P(360)$ peaks which are both sensitive to the presence of colonies on the filter, and which are therefore the best indicators of *Trichodesmium* abundance. It must be also noted that the high package effect of absorption by *Trichodesmium* colonies due to a double shadow effect of absorption of light inside the filament, and because of the stacking in a colony (Subramaniam et al., 1999; McKinna, 2015), tend to lower the specific absorption $a_P(440)$. Similarly, it was also striking that the in situ red fluorescence signal in the upper

15 layer at OUTPACE is weak as already found on CTD profiles in the region (DIAPALIS; Tenorio et al., 2018) despite a large abundance of $FTL-Tricho$. This can be attributed to a low red fluorescence of colonies in the upper layer. Also, the small volume (0.25 mL; Neveux et al., 2010) "seen" by the ECOFLNTU fluorometer of the CTD does not contain many colonies, and the response of large colonies to the blue excitation light is low comparatively to the one of the numerous small picoplanktonic cells. Such low responses in absorption and fluorescence could lead to an underestimate of the biomass of *Trichodesmium* from

20 optical remote sensing.

Backscattering in the ocean is rather influenced by small particles (< 0.5 μm) of mineral origin, bubbles and colloids than by marine living particles (Loisel et al., 2007; Stramski et al., 2008) but also by large *Trichodesmium* colonies or associated detritus (Dupouy et al., 2008). Recent studies in the open ocean indicate a greater contribution of phytoplankton-sized particles to b_{bp} than theoretically predicted (Dall'Olmo et al., 2009; Brewin et al., 2012; Martinez-Vicente et al., 2013; Slade and

25 Boss, 2017). In oligotrophic waters of the South East Pacific, absorption and backscattering coefficients are well related to TChla with specific relationships (Morel et al., 2007; Huot et al., 2008; Bricaud et al., 2010). At 5-m depth, the OUTPACE H6-backscattering data [$b_{bp}(550)$] were, in average for all stations, 2 times higher than the $b_{bp}(550)$ calculated from TChla from the equation: $b_{bp} = \sigma$ [Chl]β during BIOSOPE (Huot et al., 2008; Stramski et al., 2008). The particulate backscattering was enhanced in the presence of *Trichodesmium* with a value 2 to 5 times higher at 5-m than at 25-m depth with high Chl-

30 specific backscattering coefficients (0.006 to 0.016 m^2(mg TChla)$^{-1}$ and low backscattering slopes (as already shown in tanks; Dupouy et al., 2008). Nevertheless, the layer of the highest backscattering coefficient is situated above the 10 m-FTL_{Tricho} and no relationship was found between vertical distributions of b_{bp}, and FTL_{Tricho}, at least in the MA (SD1- SD6, LDA).

4.2 Contribution of *Trichodesmium* spp. to TChla

All *Trichodesmium* abundance data, obtained from UVP5, pigments, and flow cytometry data, or from visual counts showed a highest abundance in the western part of the MA and a lowest abundance in the SPG, with a high value at LDB. Trichome abundance estimated from pigment algorithms were in the same range than those enumerated by microscopy in the region (at 167 °E, 21 °S, DIAPALIS data; Tenório et al., 2018). The UVP5 counted the largest colonies of the Trichodesmium population, i.e., the upper part of the colony size distribution. The factor between UVP5-FTL$_{Tricho}$ and trichome concentrations visual counts depends on the number of isolated filaments, small colonies and of the number of trichomes per colony and was defined as an "aggregation factor (AF)". This AF determined when using video recorders on *Trichodesmium* colonies varied between 400 for the highest to 50 for the lowest (Davis and McGillicudy, 2001; Guidi et al., 2012; Olson et al., 2015). The larger AF found here implies that the FTL$_{Tricho}$ represents a smaller proportion of total trichomes in the South Western tropical Pacific than at other cruises or regions. The vertical distributions of UVP5-FTL$_{Tricho}$ and trichome concentration show that *Trichodesmium* populations of both sizes were concentrated below 0 and 30m, and scarce below 50 m, which contrasts with the *Trichodesmium* distribution inferred from the nifH gene still detected below 100 m (Stenegren et al., 2018). In the South West Tropical Pacific, trichomes are generally found from 0 to 60 m (Tenório et al., 2018; Carpenter, unpublished data; Trichonesia 1 in 1998 cruise), the maximum abundance being found between 5 and 10 m depth, with a regular decrease of colonies from 5-15 m to 60 m depth. Around 180°, *Trichodesmium* colonies were located deeper than in the Melanesian region. Nevertheless, there might be enough colonies below 20 m (less visible by the satellite) to produce mats episodically, when environmental conditions are favourable, as it was often observed south of Fiji with the CZCS ocean colour sensor (Dupouy et al., 1992). On this cruise, visual counts could not detect deep green *Trichodesmium* colonies as those detected in the Coral Sea at 150 °E (Neveux et al., 2006).

Apart *Trichodesmium*, Proc was the other dominant group impacting the Chla biomass in two parts of the SWTP ocean: (1) the western part of the MA between New Caledonia and Vanuatu, also impacted by a large contribution by *Trichodesmium* and (2) the eastern part of the transect (FI) which was more oligotrophic. LDB showed a dominance of both *Trichodesmium* and Proc, with TChla proportions of *Trichodesmium*, Syn+Peuk, Microeuk, Nanoeuk, and Proc of 25, 7, 1.4, 5 and 45%, respectively.

4.3 The influence of *Trichodesmium*-CDM to UV visible water-leaving radiance

OUTPACE and BIOSOPE data show that the South West and South East Pacific surface waters exhibited similar ranges of values for $nLw(\lambda)$, $and Chla$ ($0.02 - 0.58$ and $0.02 - 1.3 mg m^{-3}$, respectively). Apart the "extreme" value of 1.3 mg m^{-3} recorded in the Peru upwelling (BIOSOPE), Chla ranges were similar during the two cruises. The fact that nLw ratios were well related to TChla in the UV domain as well as in the visible domain shows that a strong coupling exists between the UV-absorbing material and Chla. The contribution of chromophoric detrital matter (CDM = CDOM + NAP) is the sum of the total coloured detritus + dissolved absorption (Bricaud et al., 2010). During OUTPACE, high CDOM amount was associated with Trichodesmium through the formation of CDOM (mainly MAAs) from colony (Subramaniam et al., 1999a; Steinberg et al., 2004; Dupouy et

14

al., 2008). MAAs identified by their strong UV absorption at 332 and 362 nm are mainly asterina-330 and shinorine, but also minor quantities of mycosporine-glycine, porphyra-334, and palythene-360; all are present in *Trichodesmium* (Carreto et al. in Roy et al., 2011). A complete analysis of the different components of CDM implies the determination of NAP after bleaching of the filters (Bricaud et al., 2010), but this is biased because of the incomplete degradation of phycoerythrins in the case of

5   high cyanobacterial abundance Note that the MAAs absorption of alive colonies is much lower than on frozen ones (Dupouy et al., 2008), and that therefore its impact is much lower on in situ nLw values, OUTPACE and BIOSOPE data differing only in two spectral bands, the yellow-green [(nL$_w$(565))] and the blue-green [(nL$_w$(490))], according to PCA results. The PC1 axis was linked to Chla concentration for both cruises while the PC2 was linked to another optically active variable, independent of Chla for OUTPACE only. PCA shows that the variability in nL$_w$(490) and nL$_w$(565) is not totally determined by Chla, as

10   a non-negligible correlation exists between PC2 and these radiances. The fact that the relationship with PC2 is absent in the South East Pacific means that these other optical components had no influence during the BIOSOPE cruise, i.e., there is no effect of PE or particles at high Chla concentrations. Indeed, Huot et al. (2008) showed that backscattering measured during the BIOSOPE stations (between 41 °W and 173 °W) was totally linked to Chla. The relationship of nL$_w$(490) to PC2 is more difficult to interpret due to its opposite behavior between the South West (OUTPACE) and the South East (BIOSOPE) Pacific.

15   One explanation would be that in the presence of *Trichodesmium*, it is expected a higher backscattering at all wavelengths (linked to another factor than Chla) and a PE fluorescence impacting nLw at 565 nm. The fact that nL$_w$(490) is not corretated to TChla in the same way than nL$_w$(565) implies that the backscattering is not the only driving parameter, and that another optical property impacts nL$_w$(490). This could be the absorption effect by zeaxanthin (the major photoprotecting pigment, not totally correlated with Chla as shown by the PCA) or by a different accessory pigment. The signification of PC2 was explored

20   by performing a new PCA using phytoplankton group index (micro, nano and pico) as additional variables, as well as other parameters [a$_P$(330) and a$_P$(565), PE > 10 μm, UVP5-FTL$_{Tricho}$, and zeaxanthin]. New PC1 and PC2 axes explain 47 and 18% of total variance, respectively. PC1 is still linked to TChla. PC2 represents the gradient between the stations influenced by cyanobacteria and those rich in micro- and nano-phytoplankton. The relationship between PC2 and cyanobacteria (rich in Chlb or/and DV-Chlb and zeaxanthin) was inverse to that with the other groups (micro-, nano-phytoplankton)). At BIOSOPE,

25   where nLw(490) is essentially function of Chla, PC2 the zeaxanthin effect would be negligible or totally linked with the one of Chla. Our PCA indicated that the two wavelengths (490 and 565 nm) showed anomalous behavior. The latter were chosen by Westberry et al. (2005) to set an algorithm to globally map Trichodesmium high abundance with SeaWiFS satellite data. In previous published works, the spectrum obtained from an optical model of a *Trichodesmium*'s bloom at equivalent Chla concentrations that those recorded in that study (0.5 mg Chla m^{-3}) showed higher magnitudes for nL$_w$(490), nL$_w$(510) and

30   nL$_w$(565) (Subramaniam et al., 1999b) with a nL$_w$(510) greater than nL$_w$(443). Moreover, the authors points out the difficulty of direct comparisons between modeled and measured UV-visible radiance due to the uncertainties in Chla measurements or *Trichodesmium* abundance. Such spectral responses were not obtained at OUTPACE. This may explain why the model did not provide satisfactory results when applied around SWTP islands (Westberry and Siegel, 2006) where blooms are numerous as detected by TRICHOSAT particularly in summer (Dupouy et al., 2011). The reason might be that the radiance anomalies at

35   490 and 565 nm are different than expected versus TChla or *Trichodesmium* concentrations, and particularly in the case of

moderate abundance.

5 Conclusions

The OUTPACE cruise in the SWTP from 158°E to 160°W provided a unique set of simultaneous measurements of $nL_w(\lambda)$ in the UV and visible domains, pigments, and *Trichodesmium* and picoplanktonic cell abundance along the whole transect during a late summer bloom. *Trichodesmium* abundance given by the UVP5 (FTL_{Tricho}, i.e., largest colonies) with a AF of 500-700 with trichome concentration by different methods decreased from West to East and occupied the 50 m upper layer of the ocean from the MA to the FI. Such AF between large colonies and trichome concentration is indicative of aggregation processes, and is specific to all cameras towered or lowered in the ocean. *Trichodesmium* abundance was also well correlated with the absorption peak of MAA's, i.e., $a_P(330)$ and the photoprotection index [$a_P(330)/a_P(676)$], useful parameters to quantify the latter. The weak CTD-Chla fluorescence and blue absorption observed in rich *Trichodesmium* waters tend to underestimate *Prochlorococcus* abundance if used on profilers or ocean colour remote sensing, while the backscattering (high coefficient, spectral troughs) trace surface aggregations. Along the 165°E-170°W transect, *Trichodesmium* together with *Trichode* represented the major part of TChla (a mean of 40% for the whole transect at the surface, as the other groups were negligible). *Trichodesmium* contribution to TChla was the highest (60% TChla) in the Western part of the Melanesian Archipelago (around New Caledonia and Vanuatu) and regularly decreased to the East, in the vicinity of the Fiji Islands, to reach a minimum in the South Pacific gyre stations where the *Prochlorococcus* contribution to TChla was higher. Profiling *Trichodesmium*abundance from 0 to 150 m with a UVP5 allowed to detect colonies deeper south of Fiji which may produce mats more episodically than at 170°E. In the SWTP, the relationship between nLw, and Chla was generally similar to that found in the Eastern Tropical Pacific. In particular, radiance ratios were related to TChla in the visible and the UV domain interpreted as a strong coupling between the UV-absorbing CDM and Chla. The nLw values were strongly correlated to Chla except in the greenish blue and yellowish green (490 and 565 nm). These results, as well as differences in the PCA of BIOSOPE data, suggested that nLw variability in the SWTP, was influenced by other variables associated with *Trichodesmium* presence, namely a high specific backscattering coefficient, phycoerythrin fluorescence, and/or zeaxanthin absorption (related with phytoplankton group size). These wavelengths (490 and 565 nm) are often chosen in *Trichodesmium* detection algorithms. While detecting *Trichodesmium* mats (above surface) with the "red edge" is possible with MODIS (Rousset et al., this issue), the change in the UV-visible radiance detected during OUTPACE at moderate *Trichodesmium* concentrations is essential to assess true nitrogen fixation rates in the SWTP as it addresses the general case where colonies are homogeneously distributed over the first optical depth. The use of a hyperspectral profiler defining better the radiance changes linked to *Trichodesmium* and the development of an instrument detecting the whole *Trichodesmium* population, including smaller colonies or isolated trichomes are both required.

Appendix A: AOPS measurements and processing

For in-water sensors, the Full-Width Half-Maximum (FWHM) of the channels was 2 nm for 305, 325 and 340 nm, and 10 nm for 380, 412, 443, 490 and 565 nm. For in-air sensors, the FWHM of the channels was 2 nm for 305, 325 and 340 nm, 10 nm for 380 nm, and 20 nm for 412, 443, 490 and 565 nm. The MicroPro free-fall profiler was operated from the rear of the ship and deployed 20-30 m away to minimize the shadowing effects and disturbances of the ship. Surface irradiance ($E_s(\lambda)$, in $\mu W\,cm^{-2}nm^{-1}$, which is equivalent to the downward irradiance just above the sea surface, ($Ed(0+,\lambda)$), was simultaneously measured at the same channels on the ship deck using other OCR-504 sensors to account for the variations of cloud conditions during the cast. Details of cast measurements are as follows. Rejection was the case at SD6 (2nd profile), during the long duration stations LDC (2nd profile day 1, 2nd profile day 2, 1st profile day 3, 2nd profile day 5) and LDA (1st profile day 5), LDB (2nd profile day 3) an LDC (2nd profile day 1, 2nd profile day 2, 2nd profile day 5). In total, all stations were characterized by at least 1, 2 profiles and sometimes 3 profiles. Only 2 values of $nL_w(\lambda)$ at 305 nm (SD5 and SD14) showed some suspicious radiometric values among the 30 nLw profiles.

$E_d(\lambda)$ was taken from the OCR Hyperpro values from 400 to 700 nm and then integrated using the formula (Tedetti et al., 2007, eq. 1) where E_d, PAR(Z) is the downward irradiance in the spectral range of PAR at depth Z (quanta $cm^{-2}\,s^{-1}$), λ is the wavelength (nm), h is the Planck's constant ($6.63.10^{-3}4$ J.s), c is the speed of light in the vacuum ($3.108\,m\,s^{-1}$) and $E_d(Z,\lambda)$ is the downward irradiance at depth Z in $\mu W\,cm^{-2}nm^{-1}$. Downward attenuation coefficient was determined in accordance with their eq. 2, where $E_d(0-,\lambda)$ is the downward irradiance beneath the surface. Because of the wave-focusing effects leading to fluctuations in in-water irradiance near the surface, irradiance data of the first meters were omitted from the calculation and $E_d(0-,\lambda)$ was theoretically computed from deck measurements as in their equation 3, where alpha (0.043) is the Fresnel reflection albedo for irradiance from sun and sky. The diffuse attenuation coefficient for upward irradiance was determined from the slope of the linear regression of the log-transformed upward radiance versus depth in accordance with the equation between $L_u(Z1,\lambda)$ and the upward radiance [$L_u(Z2,\lambda)$] ($\mu W\,cm^{-2}nm^{-1}$] at depths Z1 and Z2 (m), respectively (Tedetti et al., 2010). As for $K_d(\lambda)$, the depth interval within the upper water column used for the $K_L(\lambda)$ determination was chosen from a visual examination of each log-transformed profile and was typically 10, 15, 20, or 30 m, depending on the stations and wave bands. The determination coefficients (r2) of the $K_L(\lambda)$ calculation were > 0.98. Water-leaving radiance ($L_w(\lambda)$ in $\mu W\,cm^{-2}nm^{-1}$ was then derived (their equation 2) where $L_u(0-,\lambda)$ is the upward radiance beneath the sea surface computed by extrapolating $L_u(Z,\lambda)$ to the sea surface from $K_L(\lambda)$ and equation (1), t (0.975) is the upward Fresnel transmittance of the air-sea interface, and n (1.34) is the refractive index of water. Normalized water-leaving radiance ($nL_w(\lambda)$in $cm^{-2}sr^{-1}$) was determined (equation 3 in Tedetti et al., 2010) by dividing the water-leaving radiance ($L_w(\lambda)$ by $E_s(\lambda)$ the surface irradiance and multiplying by $F_0(\lambda)$ the solar irradiance at the top of the atmosphere, at the mean Earth-Sun distance ($mW\,cm^{-2}$). $F_0(\lambda)$ data in the ranges 305-340 nm and 380-565 nm were used from Thuillier et al. (1997, 1998), respectively as in Tedetti et al. (2010).

References

iegala I. C., Aucan J., Desnues A., Rodier M., Dupouy C., Raimbault P., Douillet P., Hunt B., Pagano M., Clavere-Graciette A., Bonnefous A., Roumagnac M., Gasol J., Periot M., Schenkels O., Sharma P., Harlay J., Eldin G., Cravatte S., Marin F., Varillon D., Roubaud F., Jamet L., Gérard P., Goyaud A., Legrand H., Gouriou Y., and Ganachaud A.: The South Pacific Ocean Time Series (SPOT) station : a first focus on diazotrophs community, http://www.eposters.net/poster/the-south-pacific-ocean-time-series-spot-station-a-first-focus-on-diazotrophs-community, 2014

Blondeau-Patissier, D., Gower, J. F. R., Dekker A. G., Phinn, S. R., Brando V. E.:A review of ocean color remote sensing methods and statistical techniques for the detection, mapping and analysis of phytoplankton blooms in coastal and open oceans, Progress in Oceanography, 123, 123-144, 2014

Bock, N., Van Wambeke, F., Dion, M. and Duhamel, S.: Microbial community structure in the Western Tropical South Pacific, Biogeosciences Discuss., https://doi.org/10.5194/bg-2017-562, 2018.

Bonnet, S., Caffin, M., Berthelot, H., and Moutin, T.: Hot spot of N2 fixation in the western tropical South Pacific pleads for a spatial decoupling between N2 fixation and denitrification, PNAS letter, doi/10.1073/pnas.1619514114, 2017.

Borstad, G. A., Gower, J., and Carpenter, E.: Development of algorithms for remote sensing of *Trichodesmium* blooms, in E.J. Carpenter et al. (eds), Marine Pelagic Cyanobacteria: *Trichodesmium* and other Diazotrophs, 193-210, 1992.

Bracher, A., Bouman, H. A., Brewin, R. J. W., Bricaud, A., Brotas, V., Ciotti, A. M., Clementson, L., Devred, E., Di Cicco, A., Dutkiewicz, S., Hardman-Mountford, N. J., Hickman, A. E., Hieronymi, M., Hirata, T., Losa, S. N., Mouw, C. B., Organelli, E., Raitsos, D. E., Uitz, J., Vogt, M., and Wolanin, A.: Obtaining Phytoplankton Diversity from Ocean Color: A Scientific Roadmap for Future Development, Front. Mar. Sci. 4:55, 2017.

Brewin, R. J. W., Hardman-Mountford, N. J., Lavender, S. J., Raitsos, D. E., Hirata, T., Uitz, J., et al.: An inter-comparison of bio-optical techniques for detecting dominant phytoplankton size class from satellite remote sensing, Remote Sens. Environ. 115, 325–339, 2011.

Brewin, R. J. W., Dall'Olmo, G., Sathyendranath, S., and Hardman-Mountford, N. J.: Particle backscattering as a function of chlorophyll and phytoplankton size structure in the open-ocean, Optics Express, 20, 17632–17652, 2012.

Bricaud, A., Babin, M., Morel, A. and Claustre H.: Variability in the chlorophyll-specific absorption coefficient of natural phytoplankton: analysis and parametrization. J. of Geophys. Res., 100, C7, 13321-13332, 1995.

Bricaud, A., Claustre, H., Ras, J., and Oubelkheir, K.: Natural variability of phytoplanktonic absorption in oceanic waters: Influence of the size structure of algal populations, Journal of Geophysical Research, 109, C11010, 2004.

Bricaud, A., Babin, M., Claustre, H., Ras, J., and Tièche, F.: Light absorption properties and absorption budget of Southeast Pacific waters, J. of Geophys. Res., 115, C08009, 2010.

Capone, D.G., Zehr, J. P., Paerl, H. W., Bergman, B., and Carpenter, E. J.: *Trichodesmium*, a globally signicant marine cyanobacterium. Science, 276, 1221-1229, 1997.

Carpenter, E. J., O'Neil, J. M., Dawson, R., Capone, D. G., Siddiqui, P. J., Roenneberg T. and Bergman B.: The tropical diazotrophic phytoplankter *Trichodesmium*: biological characteristics of two common species. Mar. Ecol. Progr. Ser., 95, 3, 295-304, 1993.

Carpenter, E. J., Subramaniam, A., and Capone, D.G.: Biomass and primary productivity of the cyanobacterium *Trichodesmium* spp. in the tropical North Atlantic Ocean. Deep Sea Res., Part I, 51, 173–203, 2004.

Carreto, J.I., and Carignan, M. O.: Mycosporine-like amino acids: relevant secondary metabolites. Chemical and ecological aspects, Mar. Drugs, 9, 387–446, 2011.

Dall'Olmo, G.,. Westberry, T. K., Behrenfeld, M. J., Boss, E., and Slade, W. H.: Significant contribution of large particles to optical backscattering in the open ocean. Biogeosciences, 6, 947–967, 2009.

Dandonneau, Y., Gohin, F.: Meridional and seasonal variations of the sea surface chlorophyll concentration in the southwestern tropical Pacific (14 to 32°S, 160 to 175°E), Deep-Sea Research, 31, 1377-1393, 1984.

Davis, C. S., and McGillicuddy, D. J. Jr.: Transatlantic abundance of the N2-fixing colonial cyanobacterium *Trichodesmium*, Science, 312(5779), 1517–1520, 2006.

De Boissieu, Menkes, C., Dupouy, C., Rodier, M., Bonnet, S., and Frouin, R. : Phytoplankton global mapping from space with a Support Vector Machine algorithm, Proc. of SPIE Vol. 9261, 92611R, SPIE, 2014.

Dupouy, C., Loisel, H., Neveux, J., Brown, S. L., Moulin, C., Blanchot, J., Le Bouteiller, A., and Landry, M. R.: Microbial absorption and backscattering coefficients from in situ and POLDER satellite data during an El Nino–Southern Oscillation cold phase in the equatorial Pacific (180°), J. Geophys. Res., 108(C12), 8138, 2003.

Dupouy, C., Neveux, J., Dirberg, G., Röttgers, R., Tenório, M. M. B., and Ouillon, S.: Bio-optical properties of the marine cyanobacteria *Trichodesmium* spp, J. Appl. Remote Sens., 2, 1–17, 2008.

Dupouy, C., Petit, M., and Dandonneau, Y.: Satellite detected cyanobacteria bloom in the southwestern tropical Pacific. Implication for nitrogen fixation, International Journal of Remote Sens., 8, 389–396, 1988.

Dupouy C., Neveux J., Ouillon S., Frouin, R., Murakami H., Hochard S., and Dirberg, G.: Inherent optical properties and satellite retrieval of chlorophyll concentration in the lagoon and open ocean waters of New Caledonia, Mar. Pollut. Bull., 61, 503–518, 2010.

Dupouy, C., Benielli-Gary, D., Neveux, J., Dandonneau, Y. and Westberry, T.K.: An algorithm for detecting *Trichodesmium* surface bloom in the South Western Tropical Pacific, Biogeosciences, 8, 3631–3647, 2011.

Dutheil, C., Aumont, O., Gorguès, T., Lorrain, A., Bonnet, S., Rodier, M., Dupouy, C., Shiozaki, T., Menkes, C.: Modelling the processes driving *Trichodesmium* spp. spatial distribution and biogeochemical impact in the tropical Pacific Ocean, Biogeosciences Discuss., https://doi.org/10.5194/bg-2017-559, 2018.

Evers-King, H., Martinez-Vicente, V., Brewin, R. J., Dall'Olmo, G., Hickman, A. E., Jackson, T., Kostadinov, T. S., Krasemann, H., Loisel, H., Röttgers, R., Roy, S., Stramski, D., Thomalla, S., Platt, T., and Sathyendranath, S.: Validation and intercomparison of ocean color algorithms for estimating particulate organic carbon in the oceans, Front. Mar. Sci. 4:251. 10.3389/fmars.2017.00251, 2017.

Ferreira, A., D. Stramski, C. A. E. Garcia, V. M. T. Garcia, A. M., Ciotti, and Mendes, C.R.B.: Variability in light absorption and scattering of phytoplankton in Patagonian waters: Role of community size structure and pigment composition, J. Geophys. Res. Oceans, 118, 698–714, 2013.

Gordon, H. R. Normalized water-leaving radiance: Revisiting the influence of surface roughness, Appl. Opt., 44, 241 – 248, doi:10.1364/AO.44.000241, 2005.

Gower, J., King, S., and Young, E.: Global remote sensing of*Trichodesmium*. International Journal of Remote Sensing, 35, 5459-5466, 2014.

Grob, C., O. Ulloa, O., H. Claustre, H., Y. Huot, Y., G. Alarcón, G. et al.. Contribution of picoplankton to the total particulate organic carbon concentration in the eastern South Pacific. Biogeosciences, 4 (5), pp.837-852, 2017.

Guidi, L., Calil, P. H. R., Duhamel, S., Björkman, K. M., Doney, S. C., Jackson, G. A., Li, B., Church, M. J., Tozzi, S., Kolber, Z. S., Richards, K.J., Fong, A. A., Letelier, R. M., Gorsky, G., Stemmann, L., and Karl, D. M.: Does eddy-eddy interaction control surface phytoplankton distribution and carbon export in the North Pacific Subtropical Gyre ? J. Geoph. Res., 117, G02024, doi:10.1029/2012JG001984, 2012.

Higgins, H. W., Wright, S. W., and Schluter, L.: Quantitative Interpretation of Chemotaxonomic Pigment Data, Chapter 6, Phytoplankton Pigments: Characterization, Chemotaxonomy and Applications in Oceanography, Suzanne Roy, Einar Skarstad Egeland, Geir Johnsen and Carole Anne Llewellyn (eds.) Cambridge University Press, 2011.

Hooker, S. B., L. Clementson, C. S. Thomas, et al.: The Fifth SeaWiFS HPLC Analysis Round-Robin Experiment (SeaHARRE-5). NASA Technical Memo. 2012-217503 NASA Goddard Space Flight Center, Greenbelt, Maryland, 98, 2012.

Hu, C., Cannizzaro, J., Carder, K. L., Muller-Karger, F. E., and Hardy, R.: Remote detection of *Trichodesmium* blooms in optically complex coastal waters: Examples with MODIS full-spectral data. Remote Sensing of Env., 114(9): 2048–2058, 2010.

Huot, Y., Morel, A., Twardowski, M. S., Stramski, D., and Reynolds, R. A.: Particle optical backscattering along a chlorophyll gradient in the upper layer of the eastern South Pacific Ocean, Biogeosciences, 5, 495–507, 2008.

Kirk, T.O.: Light and Photosynthesis in Aquatic Ecosystems, Cambridge University Press, Nature - 509 pp, 1994.

Lantoine, F, and Neveux, J.:Spatial and seasonal variations in abundance and spectral characteristics of phycoerythrins in the Tropical Northeastern Atlantic Ocean. Deep-Sea Res I 44 (2): 223-246, 1997.

Laurion, I., and Roy, S.: Growth and photoprotection of natural and enhanced ultraviolet-B radiation, growth and photoprotection in three dinoflagellates (including two strains of Alexandrium Tamarense) and one diatom exposed to four weeks of natural and enhanced ultraviolet-N radiation. Journal of Phycology, 45, 1, 16–33, 2009.

Laviale, M., and Neveux, J.: Relationships between pigment ratios and growth irradiance in 11 marine phytoplankton species, Mar. Ecol. Prog. Ser., 425:63-77, 2011.

Loisel H., Meriaux, X., Berthon, J. F., and Poteau, A.: Investigation of the optical backscattering to scattering ratio of marine particles in relation to their biogeochemical composition in the eastern English Channel and southern North Sea, Limnol. Oceanogr., 2, 739-752, 2007.

Le Bouteiller, A., Blanchot, J., and Rodier, M.: Size distribution patterns of phytoplankton in the western Pacific: towards a generalization for the tropical open ocean, Deep-Sea Res. Part A. 39, 805–823, 1992.

Martinez-Vicente, V., Dall'Olmo, G., Tarran, G.A., Boss, E.B., and Sathyendranath, S.: Optical backscattering is correlated with phytoplankton carbon across the Atlantic Ocean. Geophys. Res. Lett., 40. 1-5, 2013.

McKinna, L. I. W., Furnas, M. J., and Ridd, P. V.: A simple, binary classification algorithm for the detection of *Trichodesmium* spp. within the Great Barrier Reef using MODIS imagery, Limnol. Oceanogr. Methods, 9, 50–66, 2011.

McKinna, L. I. W.: Three decades of ocean-color remote-sensing *Trichodesmium* spp. in the World's oceans: a review, Progress in Oceanography, 131, 177-199, 2015.

Mitchell, G.: Algorithms for determining the absorption coefficient of aquatic particulates using the quantitative filter technique (QFT), in R. Spinrad (Ed), Ocean Optics 10, SPIE, Bellingham, WA, 136-147. 1990.

Mobley, C. D.: Light and Water: Radiative Transfer in Natural Waters, Academic Press, San Diego, Calif., 1994.

Morel A., and Maritorena, S.: Bio-optical properties of oceanic waters: A reappraisal. J. Geophys. Res., 106, 7163–7180, 2001.

Morel A., Gentili, B., Claustre, H., Babin, M., Bricaud, A., Ras, J., and Tieche, F.: Optical properties of the "clearest" natural waters, Limnol. Oceanogr., 52(1), 217-229, 2007.

Moutin, T., Doglioli, A. M., de Verneil, A., and Bonnet, S.: Preface: The Oligotrophy to the UlTra-oligotrophy PACific Experiment (OUTPACE cruise, 18 February to 3 April 2015), Biogeosciences, 14, 3207-3220, https://doi.org/10.5194/bg-14-3207-2017, 2017.

Neveux, J., Lantoine, F., Vaulot, D., Marie, D., and Blanchot, J.: Phycoerythrins in the southern tropical and equatorial Pacific Ocean: evidence for new cyanobacterial types, J. Geophys. Res., 104, 3311-3321, 1999.

Neveux, J., Tenorio, M. M. B., Dupouy, C., and Villareal, T.: Spectral diversity of phycoerythrins and diazotrophs abundance in tropical South Pacific, Limnol. Oceanogr., 51, 4, 1689–1698, 2006.

Neveux, J., Lefebvre, J-P, Le Gendre R., Dupouy, C., Gallois F., Courties C., Gérard P., Ouillon, S., and Fernandez, J.M. : Phytoplankton dynamics in New-Caledonian lagoon during a southeast trade winds event. Journal of Marine Systems, 82(4), 230-244, 2010.

Olson, E. M McGillicuddy, D. J. Dyhrman, S. T. Waterbury, J. B., Davis, C. S., and Solow, A. R.: The depth-distribution of nitrogen fixation by *Trichodesmium* spp. colonies in the tropical–subtropical North Atlantic, Deep-Sea Res. Part I, 104, 72-91, 2015.

Picheral, M., Guidi, L., Stemmann L., Karl, D. M., Iddaoud G. and Gorsky, G.: The Underwater Vision Profiler 5: An advanced instrument for high spatial resolution studies of particle size spectra and zooplankton, Limnol. Oceanogr. Methods, 8, 2010, 462–473, 2010.

Ras J., Uitz, J., and Claustre, H.: Spatial variability of phytoplankton pigment distributions in the Subtropical South Pacific Ocean: comparison between in situ and modelled data. Biogeosciences, 5, 353-369, 2008.

Rousselet, L., de Verneil, A., Doglioli, A. M., Petrenko, A. A., Duhamel, S., Maes, C., and Blanke, B.: Large to submesoscale surface circulation and its implications on biogeochemical/biological horizontal distributions during the OUTPACE cruise (southwest Pacific), Biogeosciences, 15, 2411-2431, https://doi.org/10.5194/bg-15-2411-2018, 2018.

Rousset, G., De Boissieu, F., Lefèvre, J., Rodier, M., Laran, S., Ridoux V., Roudault G., Gardes, L., Frouin, R., Menkes, C., and Dupouy, C.: Remote Sensing of *Trichodesmium* spp. mats in the open ocean of the Southwestern Tropical Pacific. Biogeosciences Discuss., https://doi.org/10.5194/bg-2017-571, 2018.

Sempéré, R., Para, J., Tedetti, M., Charrière, B., and Mallet, M.: Variability of Solar Radiation and CDOM in Surface Coastal Waters of the Northwestern Mediterranean Sea, Photochemistry and Photobiology, 91: 851–861, 2015.

Slade, W. H. and Boss, E.: Spectral attenuation and backscattering as indicators of average particle size, Appl. Opt., 54, 7264-7277, 2015.

Shiozaki, T., Kodama, T., and Furuya, K.: Large-scale impact of the island mass effect through nitrogen fixation in the western South Pacific Ocean, Geophys. Res. Lett., 41, 2907-2913, 2014.

Subramaniam, A., Carpenter, E. J., Karentz, D., and Falkowski, P. G.: Bio-optical properties of the marine diazotrophic cyanobacteria *Trichodesmium* spp. I- Absorption and photosynthetic action spectra, Limnol. Oceanogr., 44, 608–617, 1999a.

Subramaniam, A., Carpenter, E.J., and Falkowski, P.G.: Optical properties of the marine diazotrophic cyanobacteria *Trichodesmium* spp. II- A reflectance model for remote-sensing. Limnol. Oceanogr., 44, 618–627, 1999b.

Subramaniam, A., Brown, C. W., Hood, R. R., Carpenter, E. J., and Capone, D. G.: Detecting *Trichodesmium* blooms in SeaWiFS imagery, Deep-Sea Res. Part I, 49, 107-121, 2002.

Stramski, D., Reynolds, R. A., Babin, M., Kaczmarek, S., Lewis, M. R., et al.: Relationships between the surface concentration of particulate organic carbon and optical properties in the eastern South Pacific and eastern Atlantic Oceans. Biogeosciences, 5 (1), 171-201, 2008.

Tedetti, M., Sempéré, R., Vasilkov, A., Charrière, B., Nérini, D., Miller, W., Kawamura, K., and Raimbault, P.: High penetration of ultraviolet radiation in the south east Pacific waters, Geophys. Res. Lett., 34, L12610, doi:10.1029/2007 GL029823, 2007.

Tedetti, M., Charrière, B., Bricaud, A., Para, J., Raimbault, P., and Sempéré, R.: Distribution of normalized water leaving radiances at UV and visible wave bands in relation with chlorophyll a and colored detrital matter content in the southeast Pacific, J. Geophys. Res., 115, C02010, 2010.

Tenrio, M., Dupouy, C., Rodier, M., Neveux, J.: Trichodesmium and other Filamentous Cyanobacteria in New Caledonian waters (South West Tropical Pacific) during an El Niño Episode, Aquatic Microbial Ecology, 81: 219–241, 2018.

Uitz, J., Claustre, H., Morel, A., and Hooker, S. B.: Vertical distribution of phytoplankton communities in open ocean: An assessment

based on surface chlorophyll, J. Geophys. Res., 111, C08005, doi:10.1029/2005JC003207, 2006.

Westberry, T., Subramaniam, A., and Siegel, D.: An improved bio-optical algorithm for the remote sensing of *Trichodesmium* spp. blooms, J. Geophys. Res., 110, C06012, 2005.

Westberry, T. K. and Siegel, D. A.: Spatial and temporal distribution of *Trichodesmium* blooms in the world's oceans, Global Biogeochem. Cy., 20, 4016, 2006.
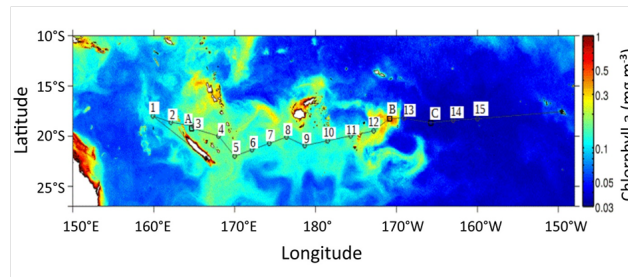
5

Figure 1. Map of chlorophyll distribution during the OUTPACE cruise (image composite of the Moderate Resolution Imaging Spectroradiometer- MODIS) data provided by CLS, Collect Localization Satellites). The positions of the 15 stations are shown by numbered squares, with A, B and C representing long duration stations (7 days), A in the Melanesian archipelago, B in the Fijian archipelago, C in the Western part of the South Pacific gyre.
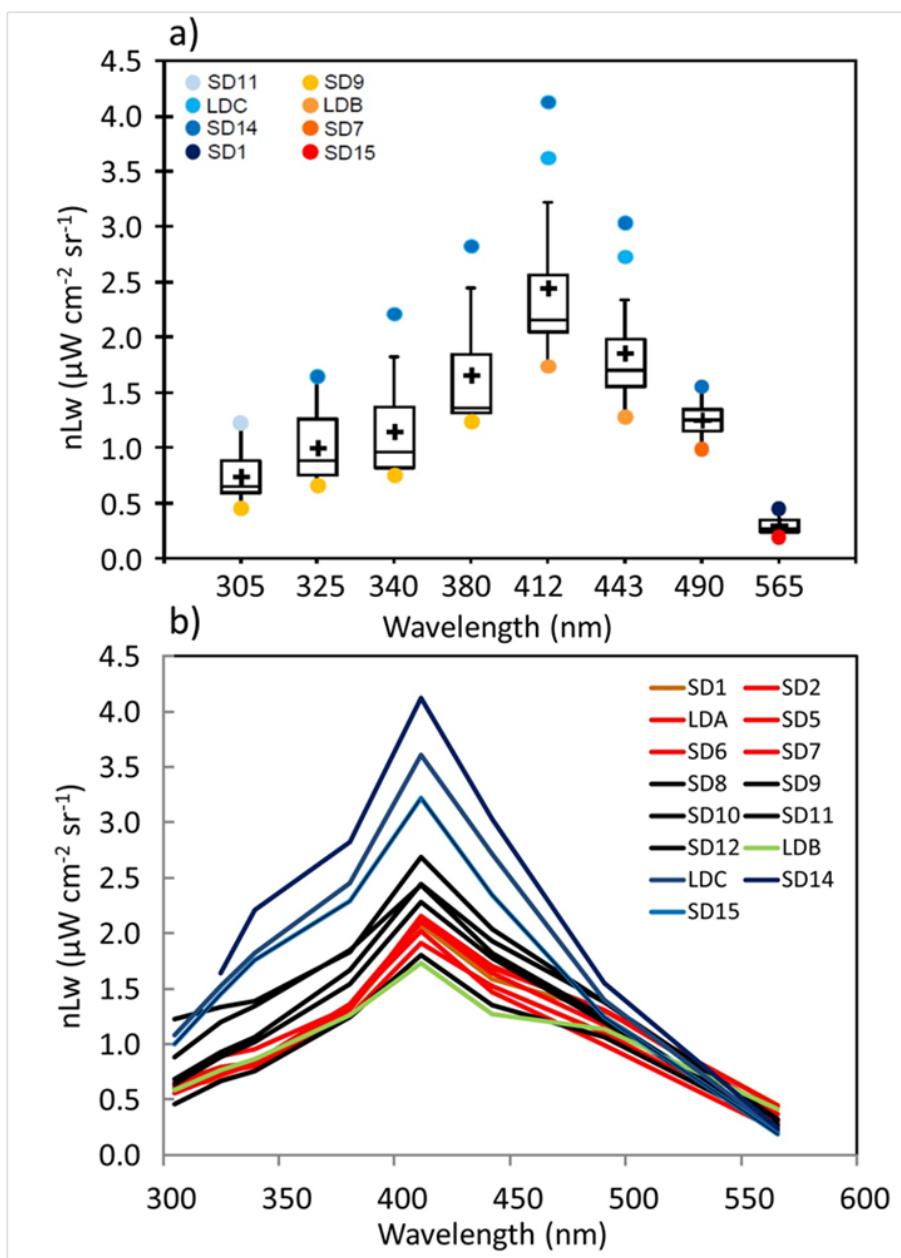
Figure 2. OUTPACE AOPs in the Western tropical South Pacific. a) Box-and-whisker plots for the distribution of $nL_w(\lambda)$ in the UV (305, 325, 340, and 380 nm) and visible (412, 443, 490, and 565 nm) spectral domains determined between 0- and 30 m at stations in the Melanesian arch. (MA, SD1-SD7 and LDA), Fijian arch. (FI, SD8-SD11), and South Pacific Gyre (SPG, SD13, LDC, SD14, SD15). The outliers stations are indicated on the upper left (see text). b) $nL_w(\lambda)$ versus wavelength with a color-code depending on TChla (in red: high concentrations $(0.185 < TChla < 0.35$ mg m^{-3} ; SD1 to SD7, Melanesian archipelago), in black: median concentrations $(0.06 < TChla < 0.1$ mg m^{-3}; SD8 to SD11 around Fiji Islands) in blue: low concentrations $(TChla < 0.11$ mg m^{-3} ; SD14 to SD15 including LDC) with the frontal station LDB in green (Table 1).
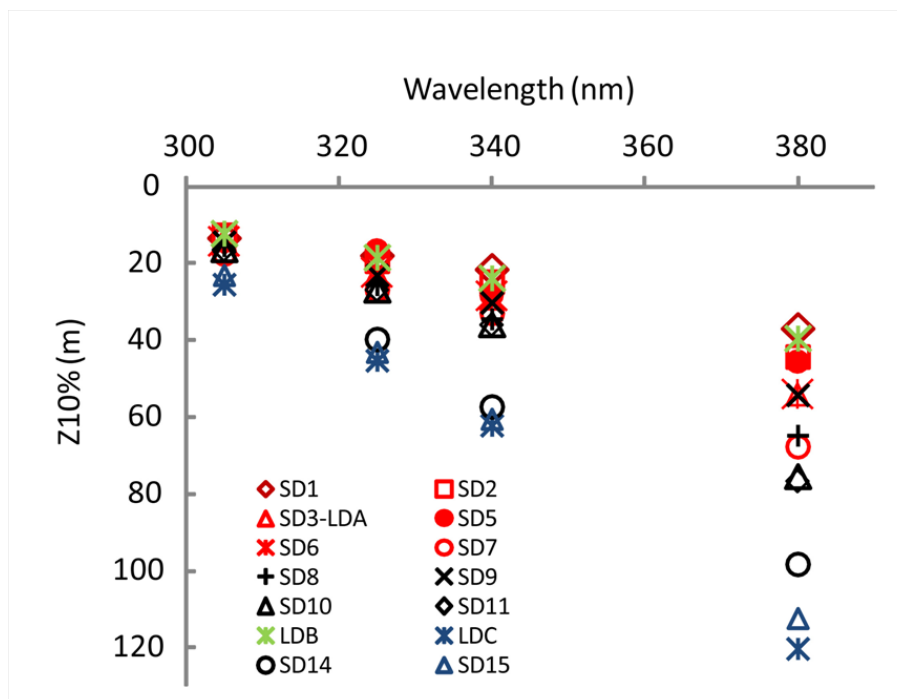
**Figure 3.** OUTPACE AOPs (continued). $Z10\%(\lambda)$ at 305 nm (UV-B), and 325, 340 and 380 nm (UVA-A) at all stations during OUTPACE in the Western tropical South Pacific with a color-code depending on TChla (in red: high concentrations ($0.185 <$ TChla < 0.35 mg m^{-3}; SD1 to SD7, Melanesian archipelago), in black: median concentrations ($0.06 <$ TChla < 0.1 mgm^{-3}; SD8 to SD11 around Fiji Islands) in blue: low concentrations (TChla < 0.11 mg m^{-3}; SD14 to SD15 including LDC) with the frontal station LDB in green (Table 1).
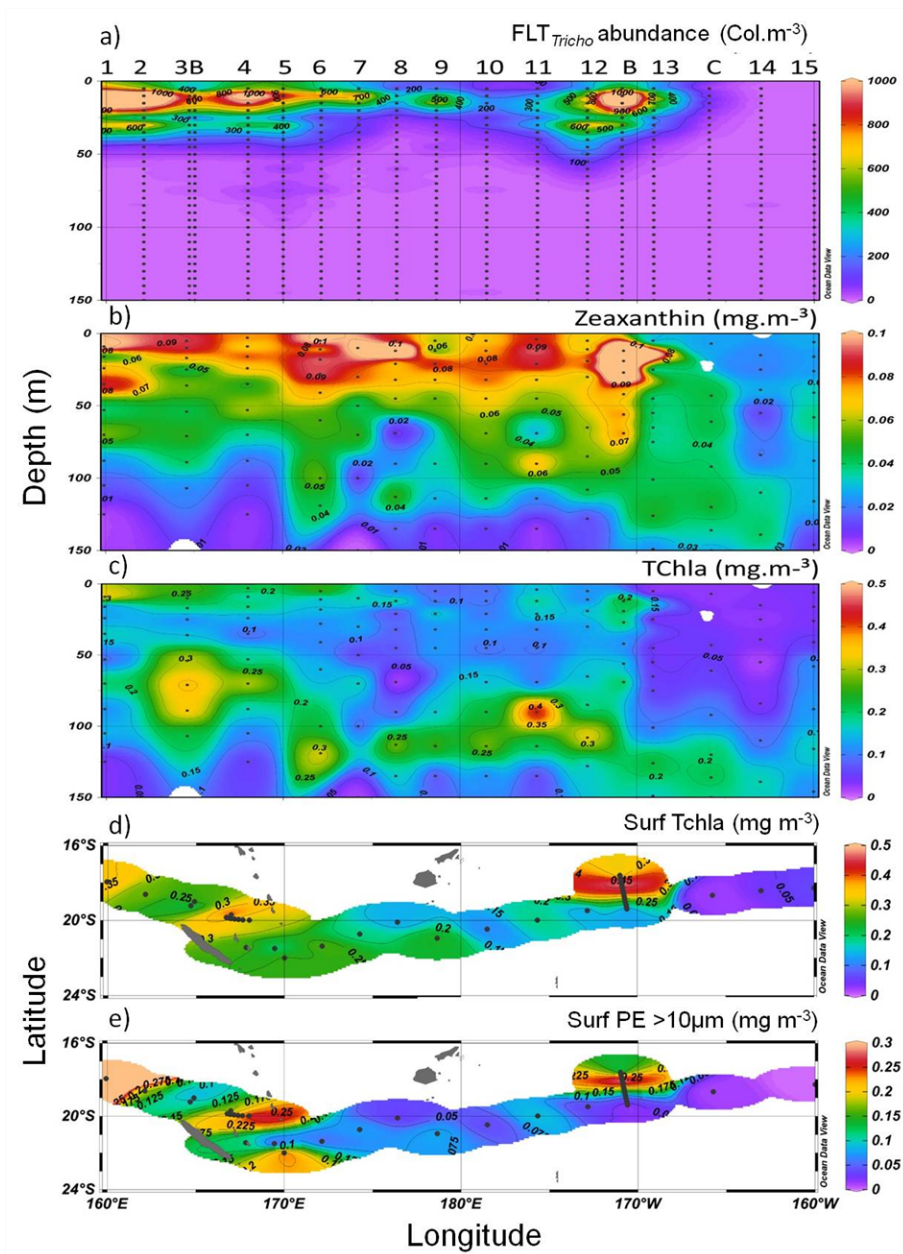
Figure 4. Sections from 0 to 150 m of a) Abundance of FTL_{Tricho} (N.m^{-3}), b) Zeaxanthin and c) TChla concentration (mg.m^{-3}) measured by HPLC- Surface maps of d) TChla and e) PE > 10 μm (mg.m^{-3}). Short transects Tchla HPLC NASA data from pump samples (sampling at 3.2 m depth) at 165°E and 170°W are included in the mapping. Ocean Data View sections Schlitzer, R., Ocean Data View, http://odv.awi.de, 2016. Station positions are indicated by black circles.
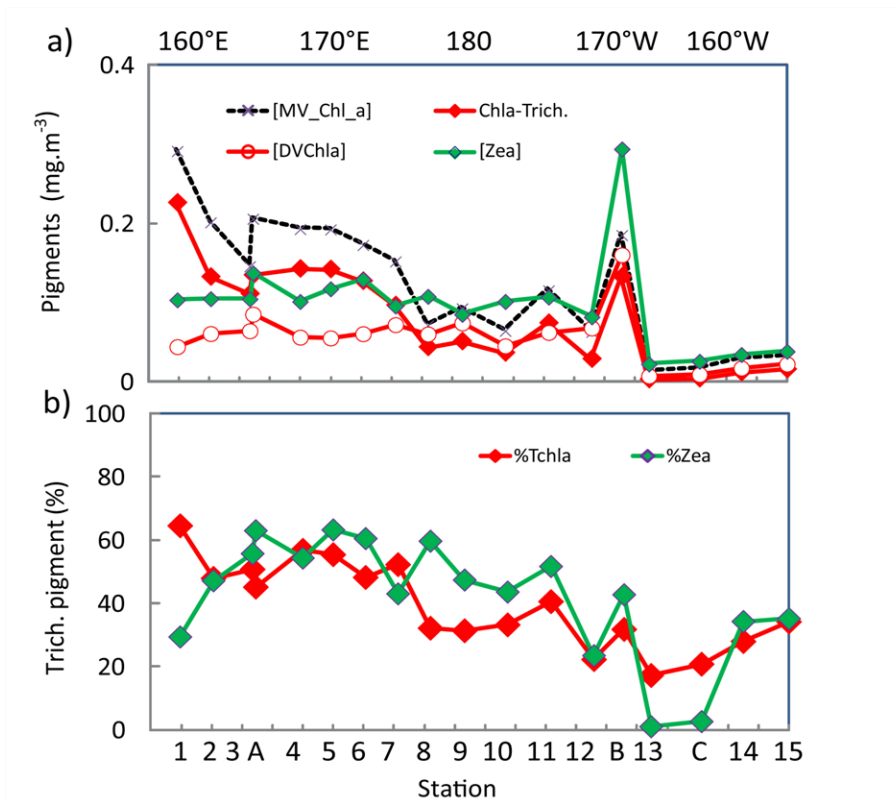
Figure 5. a) Surface concentrations (mg m^{-3}) along the OUTPACE transect of DV-Chla, total Zeaxanthin, total MV-Chla and MV-Chla related to *Trichodesmium* (Trich.) as obtained by appliance of pigment algorithms (see material and methods), b) Contribution of *Trichodesmium* to TChla and Tzeaxanthin (%). Pigments were analysed by HPLC at NASA. X axis represented station number (below) and main longitudes (above).
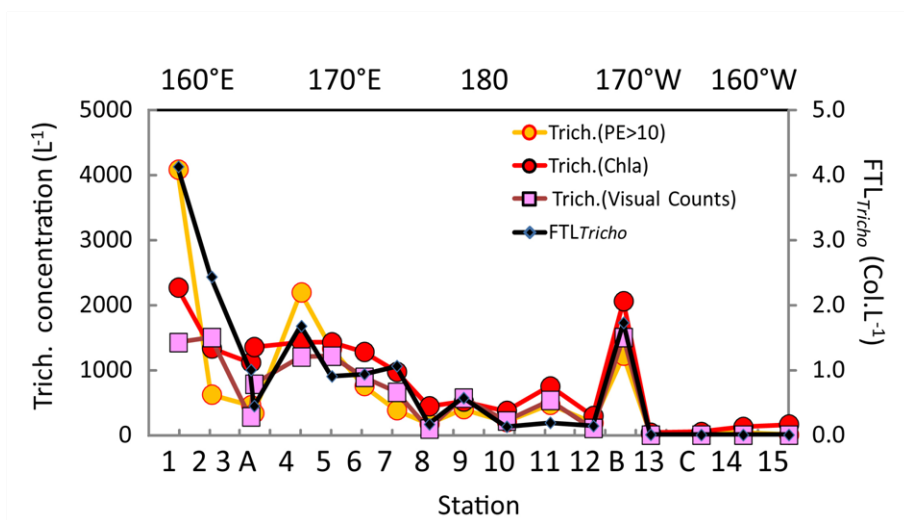
Figure 6. Surface values along the OUTPACE transect of the *Trichodesmium* abundance, in terms of trichome L^{-1} (left axis), deduced from different methods: 1) visual counts, 2) pigment algorithms using TChla (Trich.(Chla), TZeaxanthine Trich(zea) or Phycoerythrin in the > 10 μm fraction Trich.(PE > 10 μm). Comparison with FTL$_{Tricho}$ abundance (colony counts in Colonies L^{-1} by UVP5 at 10 m, right axis). X axis represents the station number (below) or the main longitudes (above).
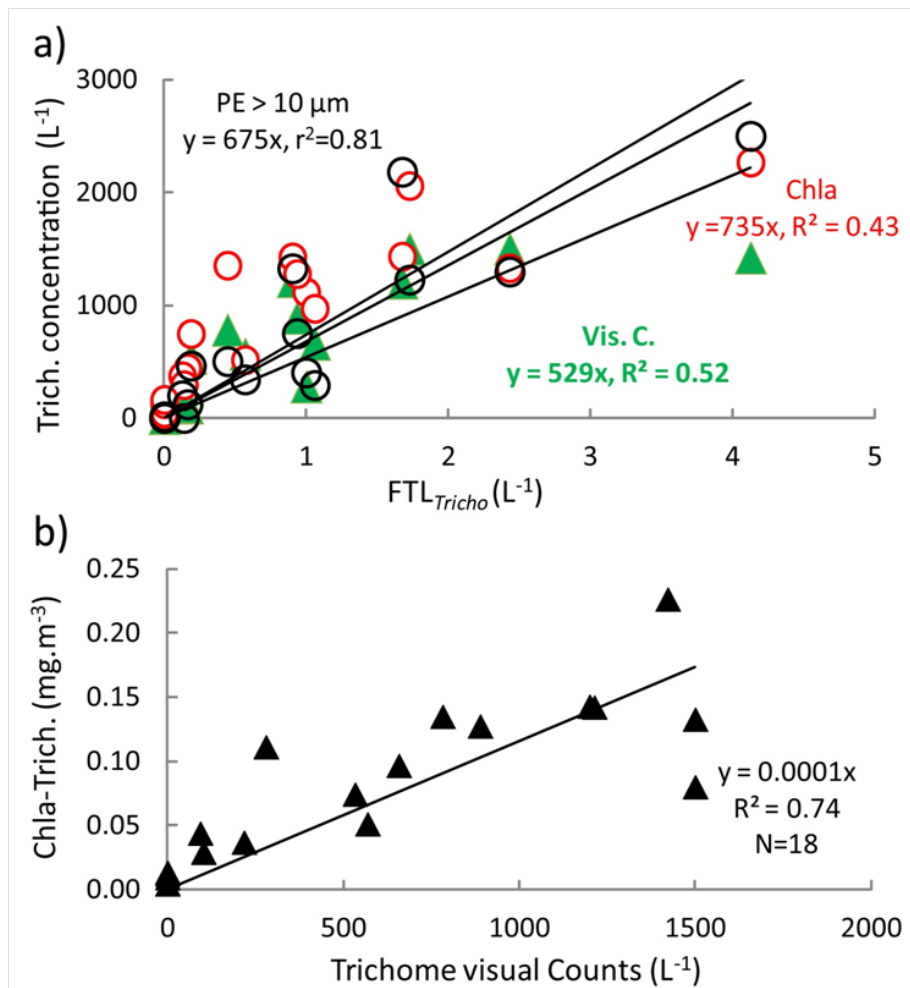
Figure 7. Correlations between the a) Trichome concentration estimated from PE > 10 μm (in black) or Chla(Tri) (in red) or visual counts (in green) and the FTL_{Tricho} abundance (colony counts by UVP5 in L^{-1}) b) Chla (Trich.) versus Trichome concentration from visual counts (Trichome L^{-1}).
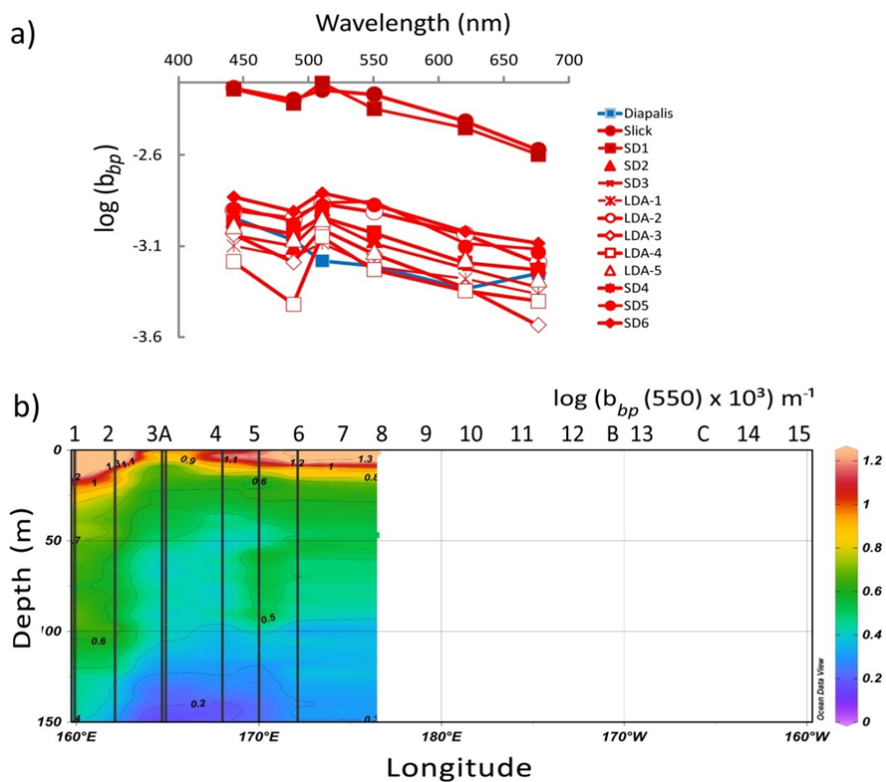
Figure 8. IOPS: a) Backscattering spectrum [log(b_{bp}inm^{-1}] vs log (wavelength) measured by a HOBILABS Hydroscat-6 in *Trichodesmium* rich waters showing troughs at the maximum absorption wavelengths (in red). Comparison with data measured at an oceanic station of the DIAPALIS 2001-2003 program (22°50 E 166°E 20) with the same H6, c) Section from 0-150m of log(b_{bp}(555)). Ocean Data View sections Schlitzer, R., Ocean Data View, http://odv.awi.de, 2016.
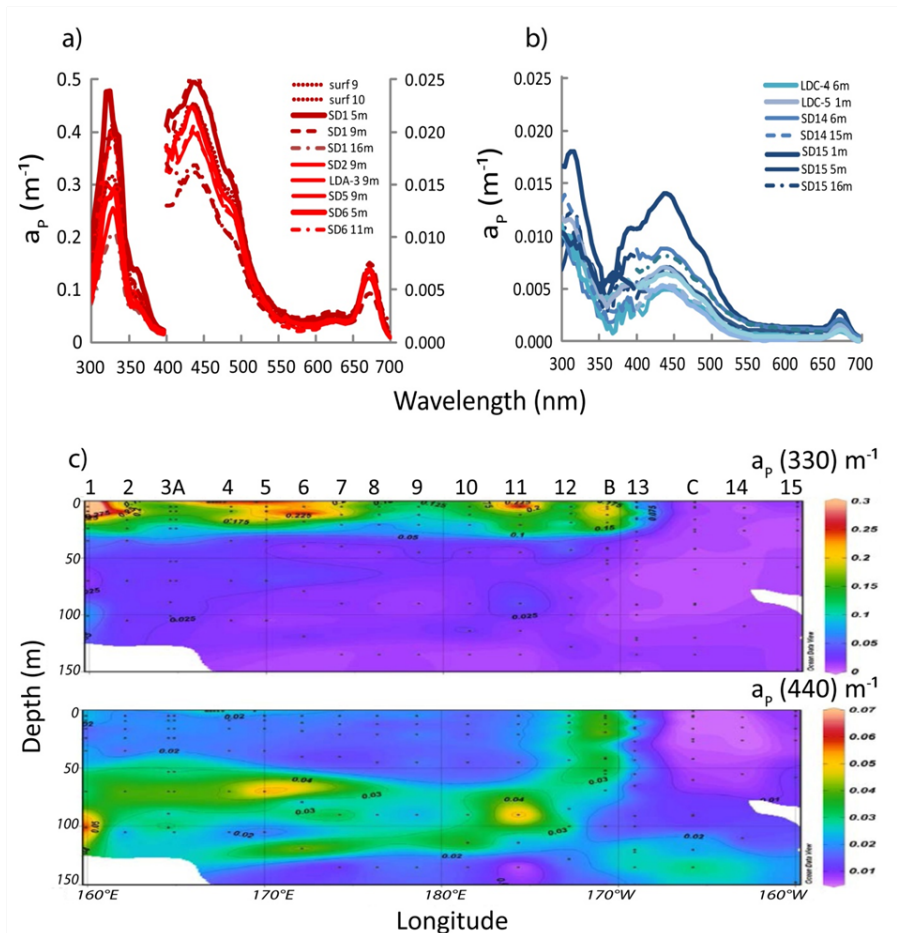
Figure 9. IOPS (continued): a) In situ absorption spectrum of *Trichodesmium* rich waters as measured by the filter technique showing MAA's absorption (on frozen filters) at 330 and 360 nm. Note the two different axis for 330nm (left Y axis) and for 440nm (right Y axis) and b) idem for *Trichodesmium* poor waters (only one Y axis), c) OUTPACE section of $a_P(330)$ (upper panel), and $a_P(440)$ (lower panel). Ocean Data View sections Schlitzer, R., Ocean Data View, http://odv.awi.de, 2016..
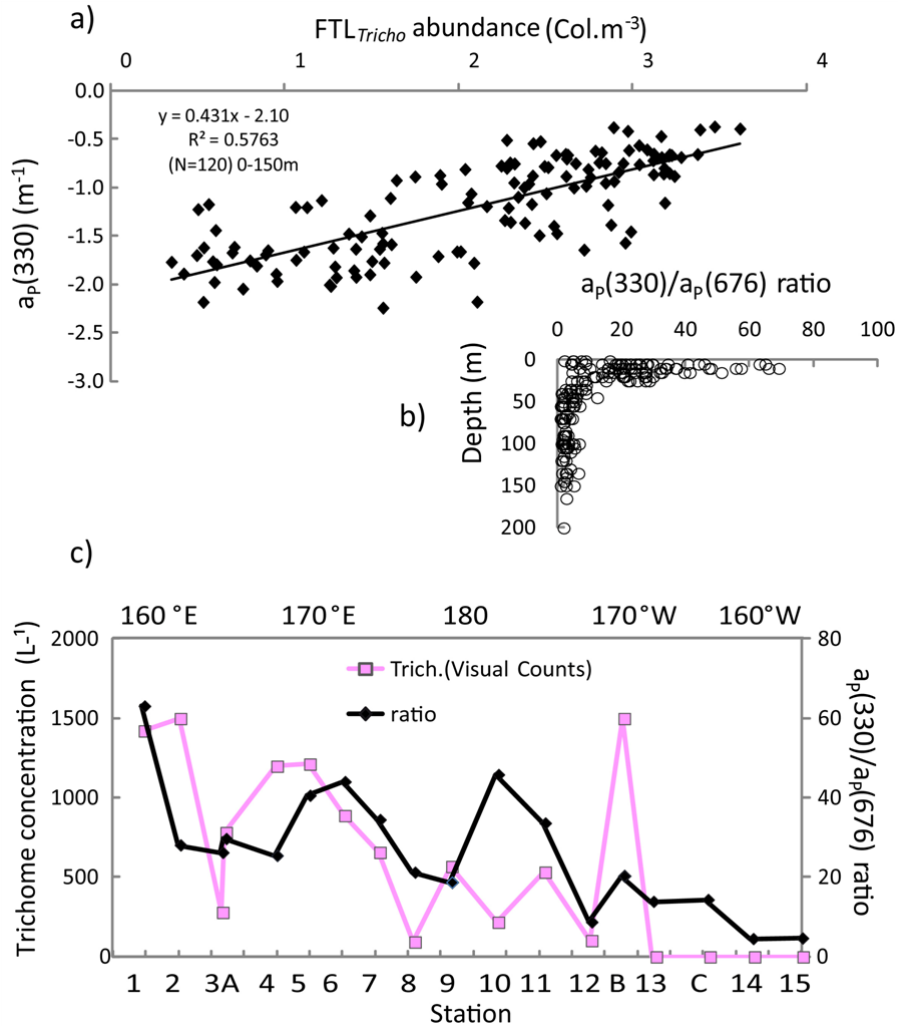
Figure 10. IOPS (continued): a) Relationship (Log/Log) between $a_P(330)$ and the UVP5 FTL_{Tricho} abundance (Colonies.m^{-3}) at all station and depths (0-150m) b) Vertical distributions of $a_P(330)$/ $a_P(676)$ at all stations, c) OUTPACE sections from 0-150m of the surface ratio $a_P(330)$/ $a_P(676)$, and trichome concentration (visual counts) along the transect. X axis represents the station numbers (below) and the main longitudes (above).
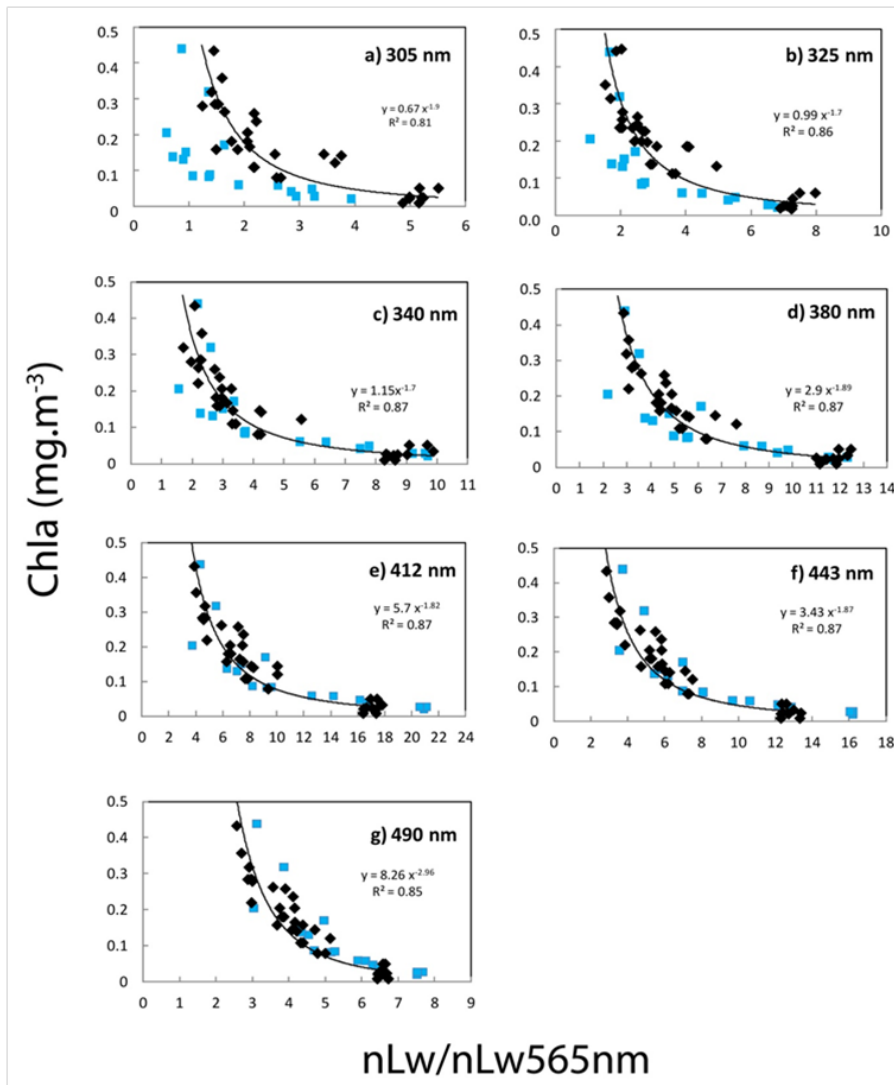
Figure 11. Correlations between the Chla (fluorimetry) and the ratio of $nL_w(\lambda)/nLw(565\ nm)$ at different UV and visible wavelengths. Equations and determination coefficient (r^2) of the power law are indicated for each wavelength a) 305, b) 325, c) 340, d) 380, e) 412, f) 443, and g) 490 nm). All stations of the OUTPACE (in black) and BIOSOPE (in blue) transect are included.

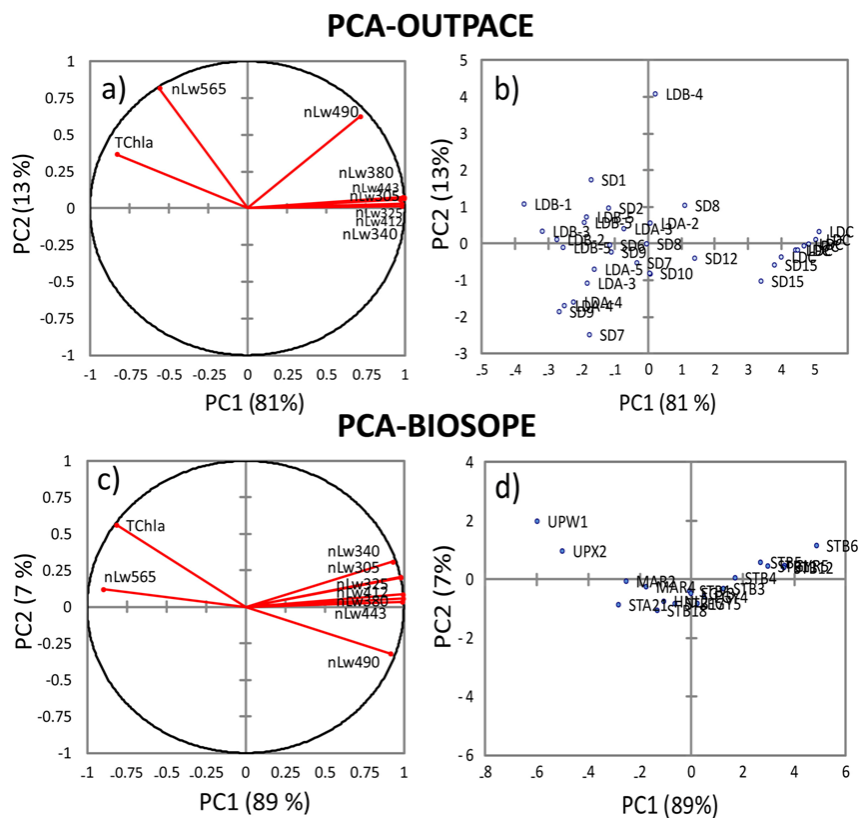**Figure 12.** Principal component analysis (PCA), based on Pearson's correlation matrices, computed on the $nL_w(\lambda)$ and TChla for OUTPACE (a, b) and for BIOSOPE (c, d). For OUTPACE (a,b) all surface data were used, including 7 days at LDA, LDB, LDC (n = 37). For BIOSOPE, all surface data (n = 17) were used (c,d). Correlation circle (left panels), projection of stations on the first factorial planes (F1 and F2) (right panels).

Station	Longitude	Latitude	Date	UT time	TChla (mg m^{-3})	FTL$_{Tricho}$ (Col.m^{-3})	DCM (m)	PE >10µm (mg m^{-3})	$K_d(\lambda)$ (m^{-1}) 305 nm	325 nm	340 nm	380 nm	PAR
SD1	159°54'E	18°00'S	21 Fev.15	20h00	0.352	4125	101	1.15	0.173	0.116	0.093	0.05	nd
SD2	162°07'E	18°37'S	22 Fev.15	21h45	0.278	2430	70	0.122	0.194	0.119	0.099	0.057	0.026
SD3	164°54'E	19°00'S	24 Fev.15	03h45	0.236	445	70	0.08	nd	nd	nd	nd	0.028
LDA*	164°41'E	19°13'S	25 Fev.15	13h00	0.220	974	100	0.10	0.074	0.041	0.029	0.012	0.024
SD4	168°00'E	20°00'S	04 Mar.15	08h30	0.199	1674	70	0.43	nd	nd	nd	nd	nd
SD5	170°00'S	22°00'S	05 Mar.15	05h45	0.258	902	70	0.26	nd	0.124	0.083	0.048	nd
SD6	172°08'E	21°22'S	06 Mar.15	03h15	0.265	935	130	0.05	0.159	0.108	0.087	0.044	0.025
SD7	174°16'E	20°44'S	07 Mar.15	00h00	0.186	1059	110	0.08	0.117	0.073	0.053	0.009	0.019
SD8	176°24'E	20°06'S	07 Mar.15	21h00	0.138	165	120	0.03	0.143	0.087	0.065	0.026	0.021
SD9	178°39'E	20°57'S	08 Mar.15	22h15	0.236	569	120	0.08	0.152	0.097	0.074	0.041	0.020
SD10	178°31'W	20°28'S	10 Mar.15	00h00	0.113	127	120	0.04	0.139	0.086	0.065	0.034	0.020
SD11	175°40'W	19°59'S	10 Mar.15	21h45	0.185	188	110	0.09	0.137	0.082	0.06	0.024	0.033
SD12	172°50'W	19°29'S	11 Mar.15	21h00	0.133	139	120	0.04	0.116	0.069	0.051	0.027	0.020
LDB*	170°52'W	18°14'S	15 Mar.15	23h00	0.433	2950	52	0.24	0.172	0.11	0.087	0.054	0.028
SD13	169°04'W	18°12'S	21 Mar.15	22h30	0.0357	4	125	0.00	nd	nd	nd	nd	nd
LDC*	165°45'W	18°41'S	23 Mar.15	01h00	0.0231	0.82	135	0.01	0.189	0.116	0.09	0.054	0.020
SD14	163°00'W	18°25'S	30 Mar.15	01h30	0.045	0	165	0.04	nd	0.056	0.04	0.023	0.018
SD15	160°00'W	18°16'S	31 Mar.15	00h00	0.061	0	110	0.00	0.097	0.054	0.039	0.021	0.016

Figure 13. Main characteristics of the OUTPACE stations for the Tchla concentration, PE > 10 μm, FTL$_{Tricho}$ and attenuation coefficients from the free-fall Satlantic UV radiometer. TChla: average concentrations in total chlorophyll a (monovinyl Chla + divinyl Chla) in surface waters derived from HPLC analyses, based on duplicate analyses (CV <8 %). FTL$_{Tricho}$ abundance: determined using underwater vision profiler 5 (UVP5). DCM: deep chlorophyll maximum. PE>10µm: phycoerythrin>10µm. Kd(): diffuse attenuation coefficient for downward irradiance in the UV (305, 325, 340, 380 nm) and PAR (400-700 nm) domains. (*) Values for Long Duration stations, i.e., LDA, LDB and LDC, averaged over 7 days.